FORTIFIKATORISK

AD725157

NOTAT NR. 48 / 69

ONE-DIMENSIONAL BLAST WAVE PROPAGATION

FORSVARETS BYGNINGSTJENESTE

Incl H 4

63

DISCLAIMER NOTICE

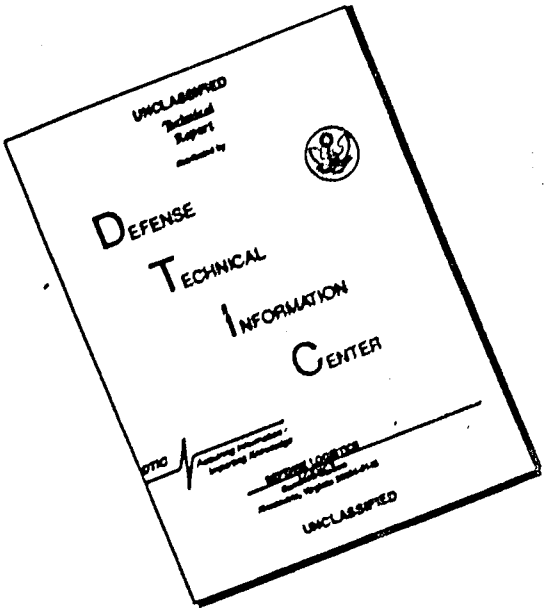

THIS DOCUMENT IS BEST QUALITY AVAILABLE. THE COPY FURNISHED TO DTIC CONTAINED A SIGNIFICANT NUMBER OF PAGES WHICH DO NOT REPRODUCE LEGIBLY.

NORWEGIAN DEFENCE CONSTRUCTION SERVICE
Office of Test and Development

Fortifikatorisk notat nr N 48/69

ONE-DIMENSIONAL BLAST WAVE PROPAGATION

by

Arne Skjeltorp

Approved:

A. Jenssen
Chief Office of Test and Development

August 1968

Acknowledgements

This is a final test report of a series of preliminary experiments concerning the feasibility of model tests used for the prediction of one-dimensional blast wave propagation. The experiments were partly supported and encouraged by the following institutions:

Grubernes Sprængstoffabriker A/S
Nitro Nobel AB (Sweden)
Norsk Sprængstofindustri A/S
Raufoss ammunisjonsfabrikker
Sprengstoffinspeksjonen

We would especially point out the efforts made by Ø. Smeby, Raufoss ammunisjonsfabrikker and K. Wenstøp, Norsk Sprængstofindustri A/S in selecting test sites, supporting explosives etc.

We also appreciate the interest and critical reading of the manuscript by Dr T.A. Zaker, Armed Services Explosives Safety Board, Washington D.C. and Mr C.A. Coulter, Ballistic Research Laboratories, U.S. Army Aberdeen Research and Development Center.

Personnel responsible for the experiments, include:

E. Berg, K. Henriksen, A.Jenssen and A. Skjeltorp, Norwegian Defence Construction Service, Office og Test and Development.

A B S T R A C T

This report is a summary of the results of a series of experiments on one-dimensional blast wave propagation in steeltubes, diameter 5 cm and 20 cm, in a concrete tube of diameter 80 cm and in a tunnel in rock of effective diameter 6 m. The blast waves originated from detonation of TNT charges placed in the center of the tubes/tunnel. Measurements of pressure time history, employing piezoelectric pressure transducers, show that frontpressure, impulse, positive duration and time of arrival scaled according to common one-dimensional scaling laws for small distances, L/D, expressed in diameter units, and for longer distances gave deviations with L/D more or less as parameter. The effects of varying wall roughness is not investigated in detail, but estimates of exponential damping constants are given.

TABLE OF CONTENTS

LIST OF ILLUSTRATIONS

LIST OF TABLES

NOMENCLATURE

C	attenuation constant defined in text
D	major inside tube/tunnel diameter
e	averaged absolute wall roughness
$e/D \cdot 100\%$	rel. wall roughness in %
I	impulse of positive pressure front
$\frac{I D^2}{Q}$	reduced impulse
k_o	scaling factor
k_1	attenuation constant defined in text
k	$D(dp/dx)/P$
l	thickness of plane charge in tube
L	distance charge-observation point
p	side-on front pressure (atm)
p_{so}	unattenuated scaled pressure
p_{20}	pressure at $L/D = 20$
$p_{av}(t)$	averaged pressure-time profile
Q	charge weight (TNT)
t_a	time of arrival of blast front
t_+	duration of overpressure

The success of any physical investigation depends on the judicious selection of what is to be observed as of primary importance, combined with a voluntary abstraction of the mind from those features which, however, attractive they may appear, we are not yet sufficiently advanced in science to investigate with profit.

J. Clerk Maxwell

I. INTRODUCTION

The need for blast load prediction methods in tunnel configurations has long been recognized. This need has become acute because of military underground defence construction projects, civil tunnel constructions for roads and water and transport-tunnels at the factories for explosives.

This report presents the results of a series of experiments on one-dimensional blast wave propagation in steeltubes, diameter 5 cm and 20 cm, in a concrete tube of diameter 80 cm and finally in a tunnel in rock of effective diameter 6 m. The blast waves originated from detonation of TNT charges placed in the center of the tubes/tunnel.

The experimental program was devoted to a study of the validity of common scaling laws and the attenuation of plane blast waves. The discussion and results are presented in rather simple terms intended to give the reader a physical picture of the phenomena which occur. The detailed discussion of the problem would be exceedingly complex and beyond the scope of this report. This report is therefore not claimed to be a strict scientific one, but rather a survey with some rules for thumb for people in charge of planning and design of constructions mentioned above.

II. S C A L I N G

II.1 Dimensional analysis

If all parts of a model have the same shapes as corresponding parts of the prototype, the two systems have geometrical similarity. There is then a point-to-point correspondance between model and prototype.

When numerical values from measurements in model are transformed to the prototype, we must consider the independent variable in the problem. A dimensional analysis of the relationship invariably leads to an equation of the form

$$(II.1) \quad a = f(a_1, a_2, \ldots\ldots\ldots a_n)$$

where the a's are a complete set of dimensionless products./1/. In most cases is it impossible to get complete similarity in a model test. Therefore we may let some of the independent variables, which are thought to be of secondary influence on the phenomenons to be investigated, diverge from their correct value.

In two systems - prototype and model - one may choose homologous cartesian systems of axis (x, y, z) and (x', y', z'). Suppose one couples the two systems together such that homologous points and times are defined by

$$x' = k_x \cdot x$$

$$y' = k_y \cdot y$$

$$z' = k_z \cdot z$$

$$t' = k_t \cdot t$$

The constants k_x, k_y and k_z are the scaling factors for the lengths in x, y and z direction. k_t is the time scaling factor.

The general expression for similarity can be defined from two abstract scalar functions f(x, y, z, t) and f'(x', y', z', t'):

It is a similarity between the functions f' and f if the ratio f'/f is a constant and the functions are evaluated at homologous points and times. The scaling factor for the function f is:

(II.3) $k_f = f'/f$

In the evaluation of scaling-laws for a system it is often useful to find:

a) The independent variables which are of importance for the experiment.

b) Perform a dimensional analysis of the variables and find invariant products.

c) Find the scaling factor for transformation from model to prototype.

II.2 The principle of similarity in one-dimensional blast wave propagation

The practical importance of the principle of similarity lies in the economy of effort it permits in determining the properties of blast waves and in the predictions it makes possible of the effect of changed scale.

Once the form of a function is found experimentally, pressure say, over a range of either distance or charge size only, its value for other weights or distances is known.

In order to check the validity of this proposition, let us change the scales of measurements of both length L_1 and time t_1 by a factor k_o, i.e. $L_2 = k_o L_1$, $t_2 = k_o t_1$. The principle of similarity asserts that the pressure and other properties of the blast wave will be unchanged if the dimensions of the charge Q are changed by the same factor k_o, or refering to fig II.1 the thickness of a plane charge in tube is changed from l_1 to $l_2 = k_o \cdot l_1$.

This is justified by the fact that the Euler equations and the Rankine-Hugoniot equations describing the blast wave if viscosity and heat conduction can be neglected, are satisfied by all sets of values of L, t and l as the scaling factor k_o cancels out as all the derivatives are of first order.

This is discussed in detail in ref /2/.

From this we may conclude that if the principle of similarity is true at any value (L_1, t_1), e.g., pressure $P(r_1, t_1) = P(k_o r_1, k_o t_1) = P(r_2, t_2)$, it is true for all values of L and t.

The validity of the principle therefore depends on whether similarity is found to hold true in the initial stages of the explosion.

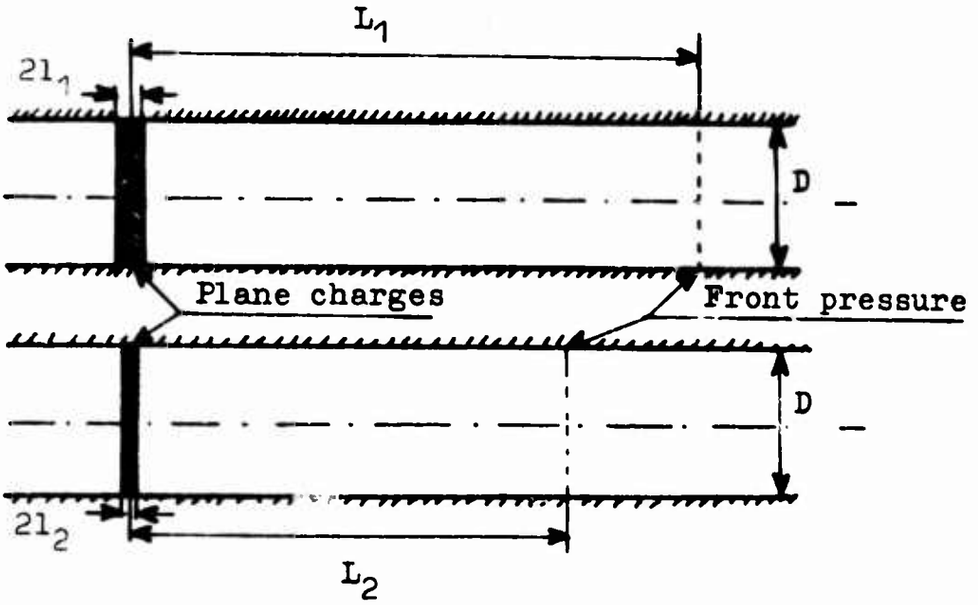

Fig II.1 Plane charges filling the whole tube cross-section

The fact that the pressure and other properties are unchanged if the linear dimensions of the source and scales of length and time are all changed in the same ratio, does not of course specify what the values are without other informations, but experiments may give the functional dependence The principle can be satisfied only if the pressure depends on distance and time only as a function of the ratios l/L, t/l and hence the frontpressure may be expressed as

$$p = f\left(\frac{l}{L}\right) \tag{II.4}$$

Another important property of such a blast wave is the impulse. For unit area of the wave front the impulse I is given by

$$I(L, t') = \int_0^{t'} p(L, t)dt \tag{II.5}$$

where the origin of time is taken to be arrival of blast front at L. The time t' to which the integration is carried out should be taken proportional

to the scaling factor and we write $t' = A \cdot l$ where A is a function only of l/L, and the pressure P depends on L and t only by the ratios l/L, t/l.

hence

$$(II.6)\quad I(L, t') = l \cdot \int_0^{A(\frac{l}{L})} p\left(\frac{l}{L}, \frac{t}{l}\right) d\left(\frac{t}{l}\right)$$

and the integral being a function only of l/L, we obtain

$$(II.7)\quad I(L, t) = l \cdot g\left[\frac{l}{L}, A\left(\frac{l}{L}\right)\right]$$

where g is an undetermined function.

The impulse measured for proportional distance and time scales is therefore proportional to the linear dimension l.

If one detonates a spherical charge, Q, in a tube, the detonation generates a blast wave which more and more gets the character of a one-dimensional wave when it propagates down the tube (fig II.3).

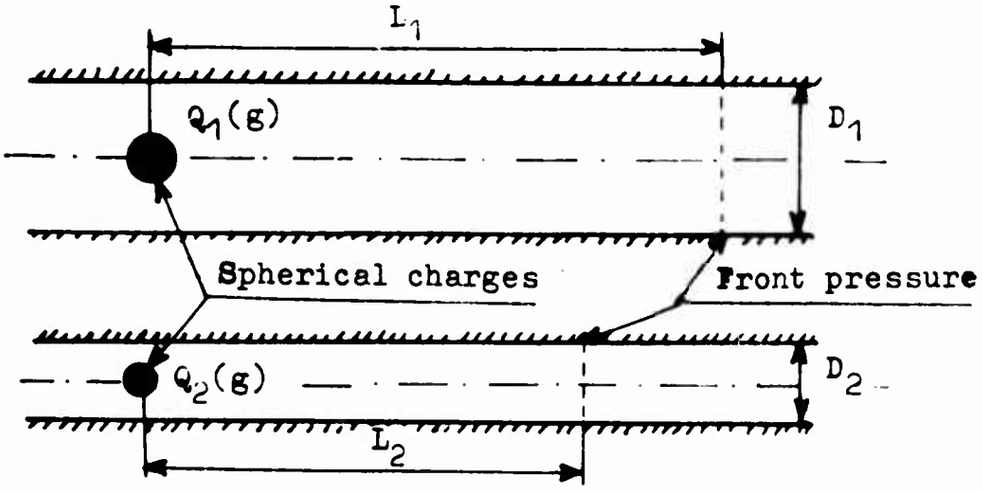

Fig II.2 Spherical charges in tubes

Since the linear dimensions of a charge are proportional to the cube root of the volume and hence weight Q the thickness l in fig II.4 is given as

(II.8) $1 \propto \frac{Q}{D^2}$

From the previous we are now prepared to write the scaling laws for the most important blast wave parameters.

(II.9) Pressure: $p = f\left(\frac{Q/D^2}{L}\right)$

(II.10) Impulse: $\frac{I}{Q/D^2} = g\left(\frac{Q/D^2}{L}\right)$

Positive duration (or duration of overpressure):

(II.11) $\frac{t_+}{Q/D^2} = h\left(\frac{Q/D^2}{L}\right)$

Arrival time of pressure front (or time from detonation to blast wave reaches distance L):

(II.12) $\frac{t_a}{Q/D^2} = i\left(\frac{Q/D^2}{L}\right)$

Here f, g, h and i are unknown function of Q/LD^2, (shortened equivalent charge weight Q_E) and may hopefully be determined by experiments.

Experiments on this has been done in Sweden ref. /3/.

II.3 Attenuation in long tunnels.

A blast wave is a physical discontinuity which is propagated through a suitable elastic fluid with a characteristic supersonic velocity M (Mach number). When the medium exhibits energy dissipative effects such as viscosity and thermal conductivity, a reduction in the magnitude of these discontinuities and an increase in the length of the discontinuous region occurs.

An added attenuation is introduced when the blast wave is confined to the interior of a bounded medium such as a tube. The added factor may be separated into two contributions, one being characteristic of the fact that the blast wave

is generated from detonation of more or less spherical charges within the tube itself, and the other being characteristic of the walls and the strength of the blast wave.

The first type of attenuation gives a pressure decrement which is very steep and is in effect the first few tube diameters in traversed distance (fig II.3).

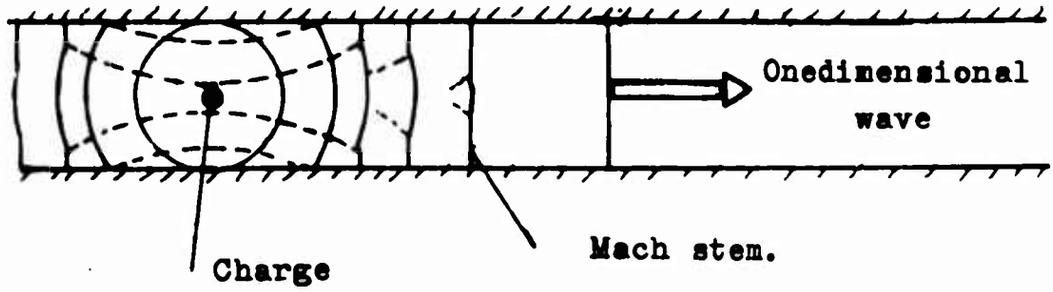

Fig. II.3. Blast wave formation inside a tube

The pressure across the shock front attenuates as it travels down the tube due also to the frictional losses on the walls of the tube. For very short tunnel lengths, i.e. for tunnels whose lengths are not very many times greater than the diameter (or its average cross-sectional diameter for the tunnel) attenuation due to wall roughness is very small. However, for long tunnels having lengths equal to about 30 or more diameters, significant attenuation of the blast wave should be expected. One of the primary aims of this program is to experimentally determine the magnitude of this attenuation.

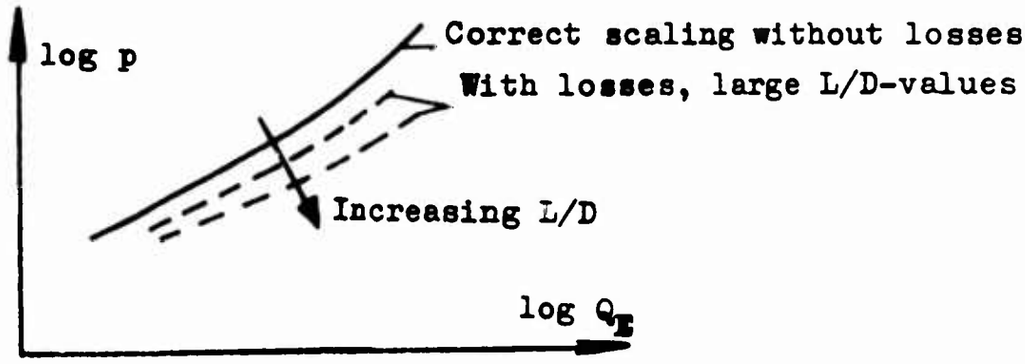

Fig. II.4. Deviation from ideal scaling.

Without wall attenuation and different other dissipative effects for different tubes/tunnels and charges, the experimental points for front pressure versus equivalent charge after eq (II.9) should lie on one smooth curve as shown in fig. II.4. Attenuation due to wall roughness would move this curve with L/D more or less as parameter for one type of tube and roughness. This comes about from principle of similarity described in part II.2, which evidently fails in any circumstances for forces not scaling geometrically. One such force is the effects of viscosity which gives rise to terms of second order derivatives in the equation of motion, and with this the equation of motion is not satisfied on substituting $p(k_oL_1, k_ot_1)$ etc for $p(L_1, t_1)$ etc.

At the last front, processes similar in effect to macroscopic viscosity and thermal conduction must be significant, but this turns out to be of no practical significance to the applicability of the principle of similarity.

For the tunnel the effective diameter is taken as $D = (4A/II)^{\frac{1}{2}}$, where A is the tunnel area. applicable for scaling of length in frictionless flow. Friction effects, however, depend on the length of the tunnel periphery C in contact with the moving gas, and the effective diameter is more properly C/II. In our case, however, the tunnel diameter was not defind better than difference between the two definitions because of somewhat varying tunnel diameter.

III. T E S T P R O G R A M

III.1 General

The tubes used were chosen as to make a rough test of the validity of common scaling laws. As our Office of Test and Development neither had the money nor the time to make extensive tests, only steeltubes of diameter 5 and 20 cm, a concrete tube of diameter 80 cm and a tunnel in rock of effective diameter 600 cm with constant roughness for each tube/tunnel were used.

General test descriptions for these series of experiments are tabulated in table III.1.

Tube/Tunnel	Steel	Steel	Concrete	Rock
Diameter D(cm)	5	20	80	600
Wall roughness e/D 100%	0,5% (e ≃ 0,26 mm)	0,13% (e ≃ 0,26 mm)	0,03% (e ≃ 0,2 mm)	8% (e ≃ 0,5 m)
Charges TNT x) (g) between	1,5-17,5	1,5-200	9,5-5000	21,5-92300
Distance charge - meas. L/D between	6,4-705,2	4,5-150,7	4,85-100,5	2,92-38,33
Side-on overpressure p(ato) between	0,2-77	0,2-32	0,07-23	0,005-1,5

x) Electrical detonation cap no 8, equivalent TNT charge 1,5 g included.

Table III.1. Test description

Fig II 5. 80 cm diameter concrete tube at test site.

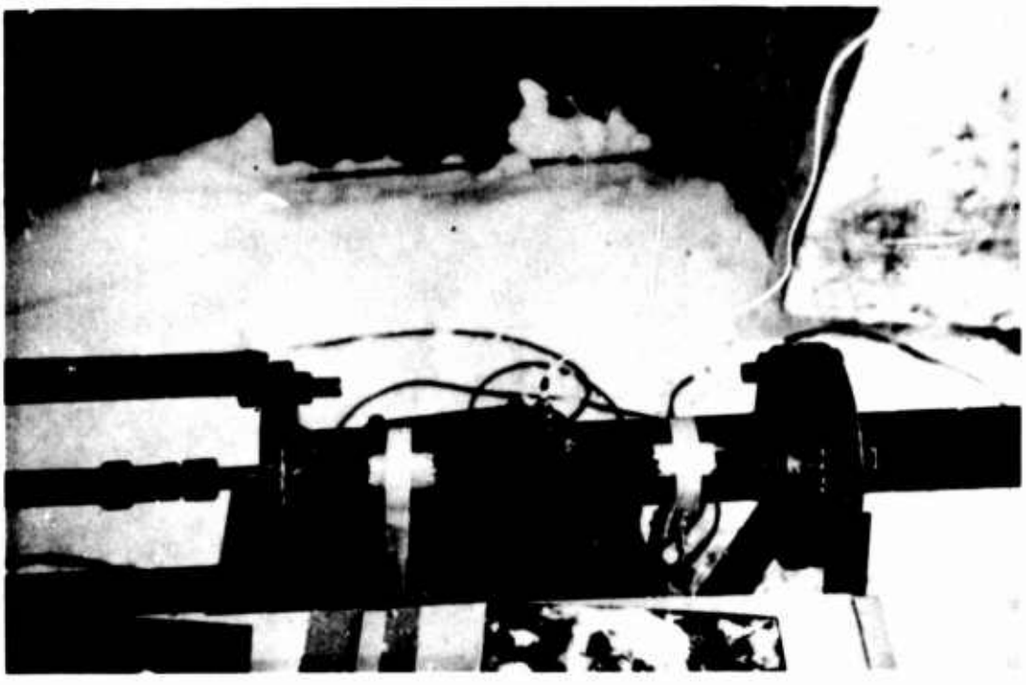

Fig II 6. 5 cm diameter steel tube with transducer mounting and arrangement for time of arrival measurements.

Pencilshaped Lead Zirconate transducers were used in conjuction with an oscilloscope and polaroid camera to measure pressure-time history. These transducers were centermounted in the tubes/tunnel.

Fig II.5 shows the 80 cm diameter concrete tube and II.6 a portion of the 5 cm diameter steel tube.

III.2 Roughness of tubes and tunnel in rock

Tunnel wall roughness was estimated by taking the percentage of the ratio e/D, where e is the roughness particle diameter and D is the tube/tunnel diameter.

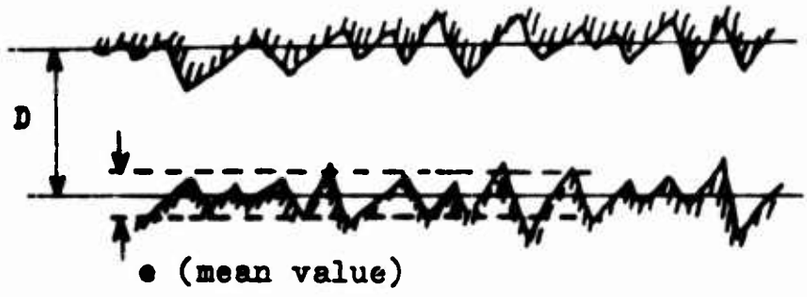

Fig.III.1. Definition of roughness $\frac{e}{D} \cdot 100\%$

As for the steeltubes the roughness originated from corrosion. For the concrete tube the roughness was the standard production roughness for PREMO-tubes, manufactured at A/S Dalen Portland-Cementfabrik, Brevik, Norway.

The tunnel used was an abandoned railway tunnel with raw-detonated rock. The tunnel had a curvature of radius approximately 100 m. It is thought that the effect of this bend can be neglected and the tunnel may be considered as being straight.

III.3 Explosive charges

The explosive used were cylindrical pressed TNT charges with a hole drilled along the cylinder-axis to fit the electrical detonation cap no 8.

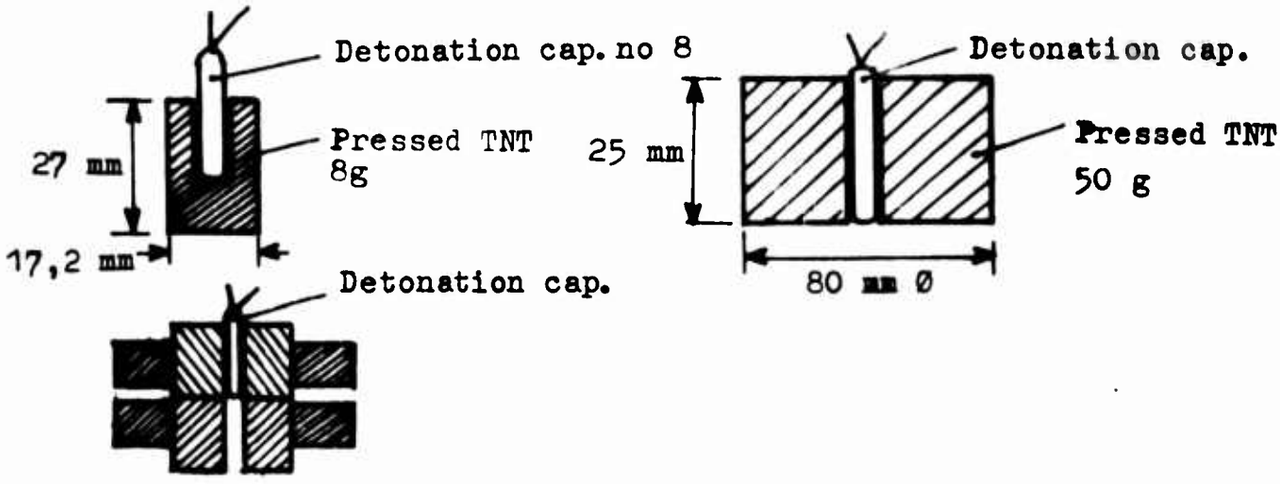

Fig III.2. Typical TNT-charges used

In a series of calibration tests the electrical detonation cap was found to be 1,5 g equivalent TNT charge as regards front pressure.

The charges were hanging in center of tube in a string going through a small hole on the upper side of the tube. In the tunnel tests the heavier charges were placed on a wooden platform as to be placed roughly in the center of the tunnel. The different shaped charges is not believed to have had any significant influence on blast waves at longer distances ($L/D \gtrsim 5$).

III.4 Transducers

The gages used were type LC-33, from Atlantic Research Corporation. This is a pencilshaped Lead Zirconate and side-on pressure measuring type transducer. The nominal characteristics in table III.2. Typical pressure time profile from test in shock tube is shown in fig.III.4.
The transducers were calibrated at the factory to within ± 1% reproducibility in the pressure range from 1,7 ato to 13.6 ato.
A best fit calibration curve was used by the computer in evaluation of frontpressure and impulse. Up to 5% uncertainty in calibration was deemed adequate in view of the larger errors introduced in interpreting the oscillographs.

Model LC-33

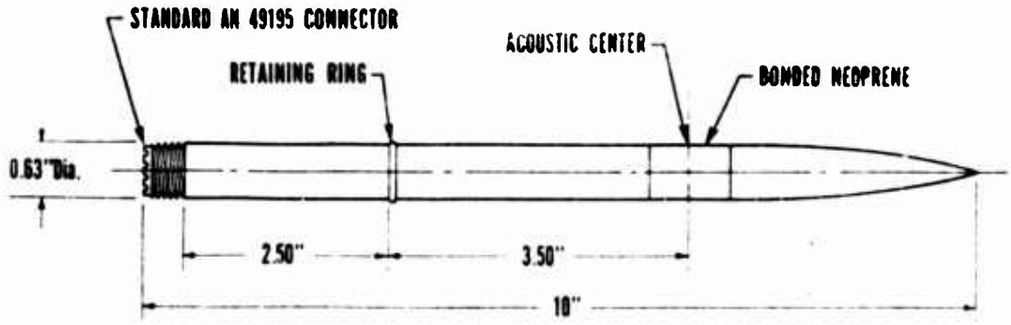

Fig III.3. Dimensions of LC-33 transducer

Table III.2

NOMINAL CHARACTERISTICS

Open Circuit Receiving Sensitivity (1 Kcps)	
db reference 1 volt/microbar	-101
Volts/psi	0.6
Charge Sensitivity (micromicrocoulombs/psi)	2500
Frequency Response, flat +2 db	1 cps to 80 Kcps
Capacitance (microfarads)	0.004
DC Resistance (megohms)	>500
Maximum Static Pressure (psi)	>500
Maximum Transient Pressure (psi)	~1000
Temperature Range (°C)	-40 to +100
Linearity	
Pressure +2% (psi)	100
Temperature +3% (°C)	-60 to +70

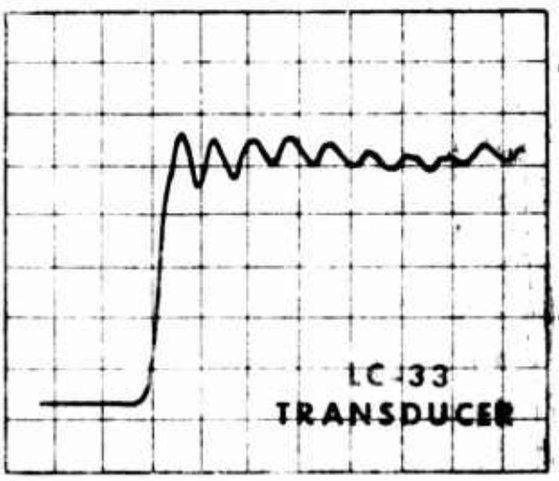

ORIENTATION. . . . FACE ON

MEDIUM. . . . . NITROGEN GAS

PRESSURE . . . . . 38 PSI

VERTICAL . . . . . 5.0 V/div

HORIZONTAL . . . . 0.02 ms/div

Fig III.4 TYPICAL PRESSURE-TIME PROFILE

III.5 Transducer mounting

The way in which the gage was mounted in the 5 and 20 cm tube is shown in fig. III.5

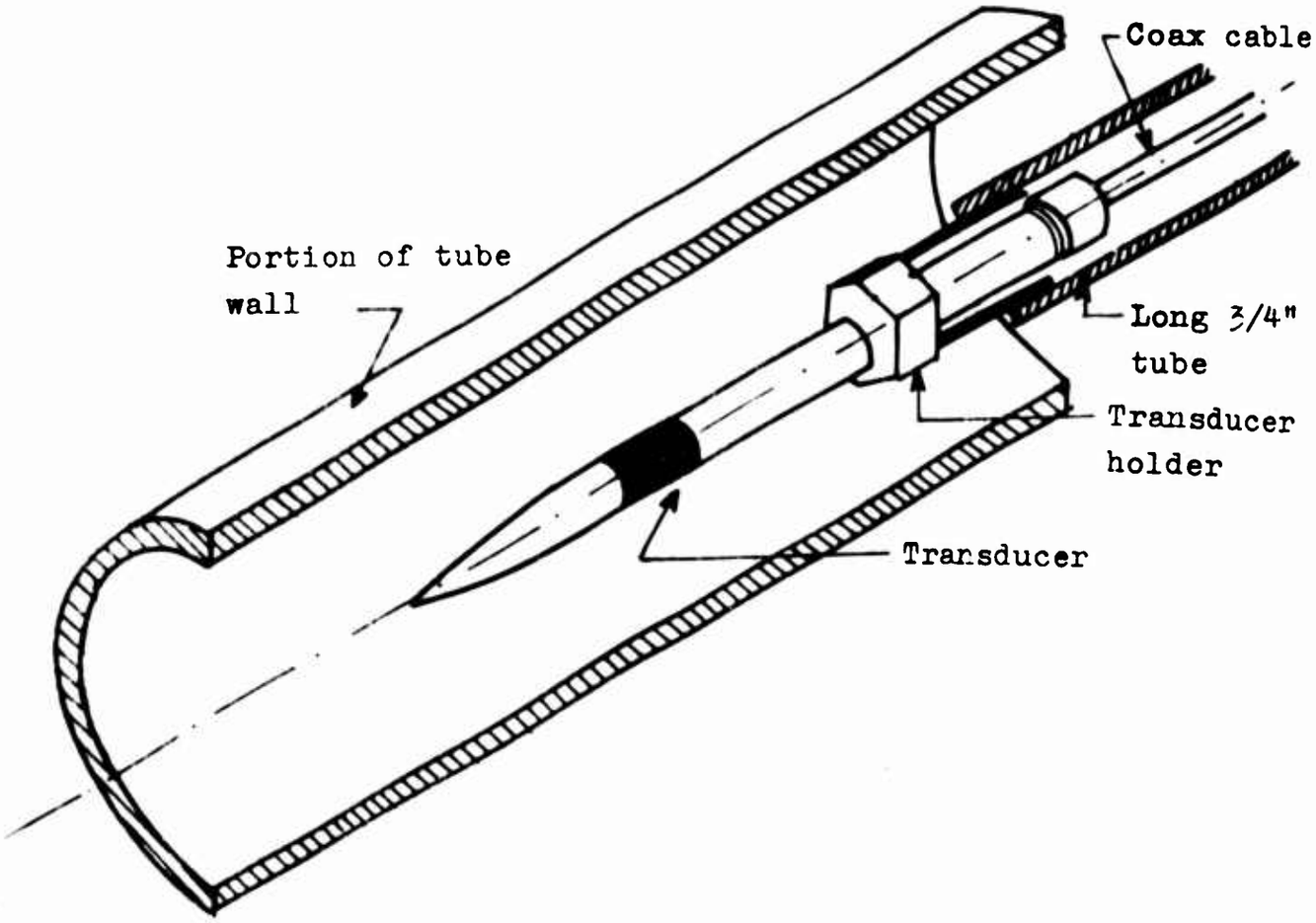

Fig.III.5. Transducer mounted in 5 and 20 cm tube

For the 5 cm and 20 cm tube only one transducer was mounted in the same tube, but as for the 80 cm tube four were mounted at the same time, fig.III.6.

The transducer body and mounting tube are of appreciable diameter compared with that of the smallest tube tested. The area constriction due to the 3/4-in. mounting tube in this case is about 14 percent. The presence of a gage can locally affect the peak pressure and impulse under these conditions.

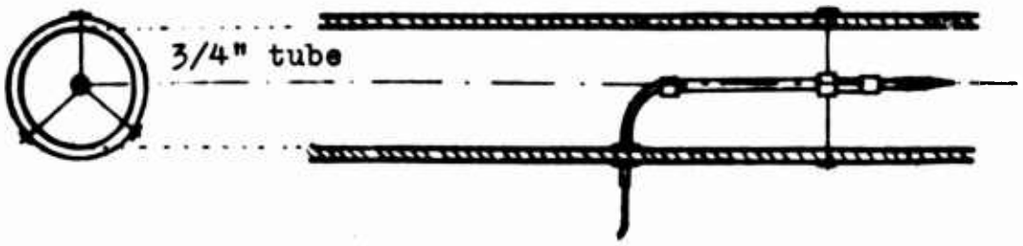

Fig III.6. Transducer mounted in 80 cm tube

In the tunnel 5 transducers were mounted at the same time as shown in fig.III.7.

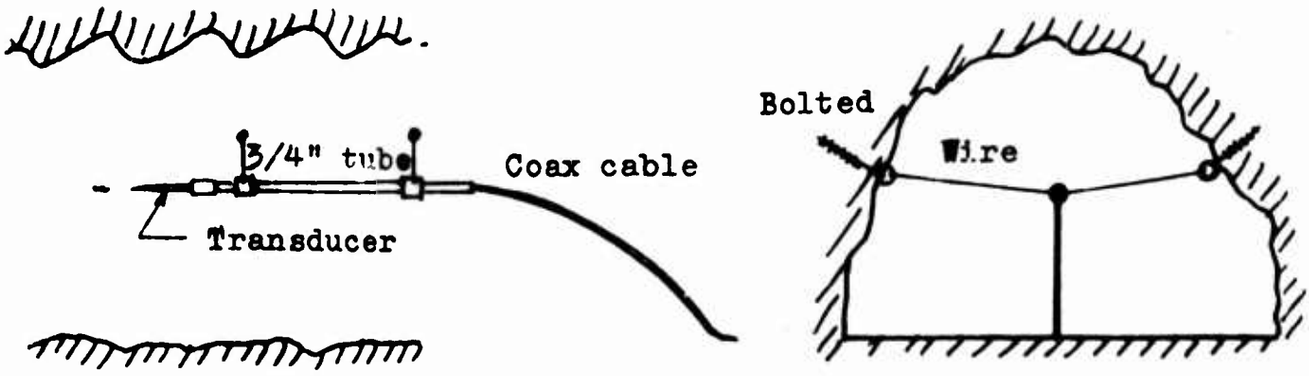

Fig III.7. Transducer mounted in 6 m tunnel in rock

III.6 Instrumentation

The electrical arrangement shown in fig III.8 was followed for the 5 and 20 cm tubes. The Kistler Charge Amplifier (Model 566) served in most cases to match the high impedance of the transducer ($> 10^8$ ohm) to the oscilloscope, a Tektronix Model 502 A. A Polaroid type oscilloscope camera recorded the trace. In many cases a large capacity served as a timeconstant increasing device.

Triggering was done by taping a loop of insulated wire around the charge. In detonating the charge, a well-defined break of wire is obtained. The uncertainty intriggeringis estimated to less then 500 μs.

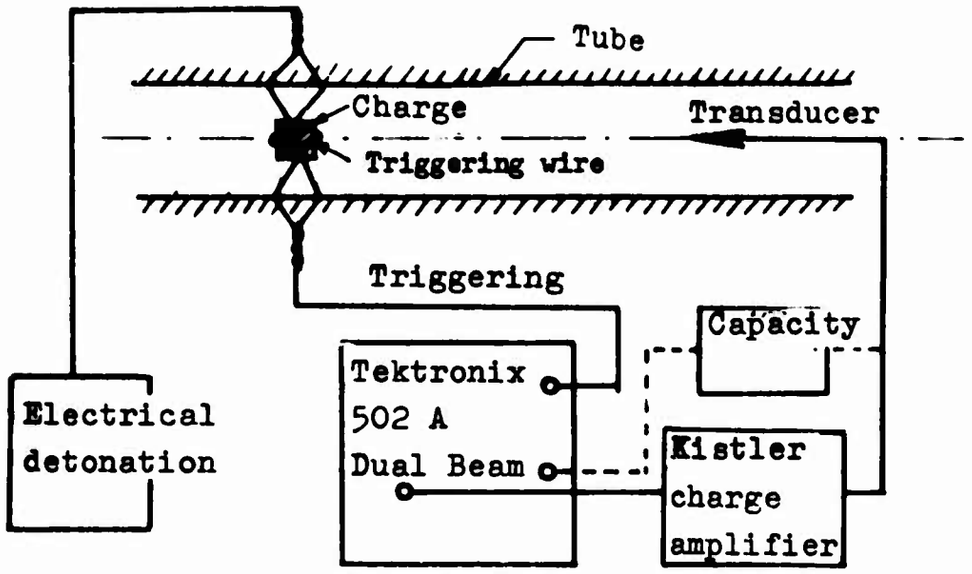

Fig III.8. Schematic electrical flow chart for 5 and 20 cm diameter tube tests

For the less transient blast waves in the 80 cm tube and 6 m tunnel, a CEC recording oscillograph (Consolidated Electrodynamics) was used with preferably fluid damped galvanometers type 7-363, fig III.9. The galvanometer has the following specifications:

Undamped natural frequency	1670 Hz
Flat (5%) frequency range	0-1000 Hz
Undamped DC sensitivity	2 mA/inch
Terminal resistance	69 ohm

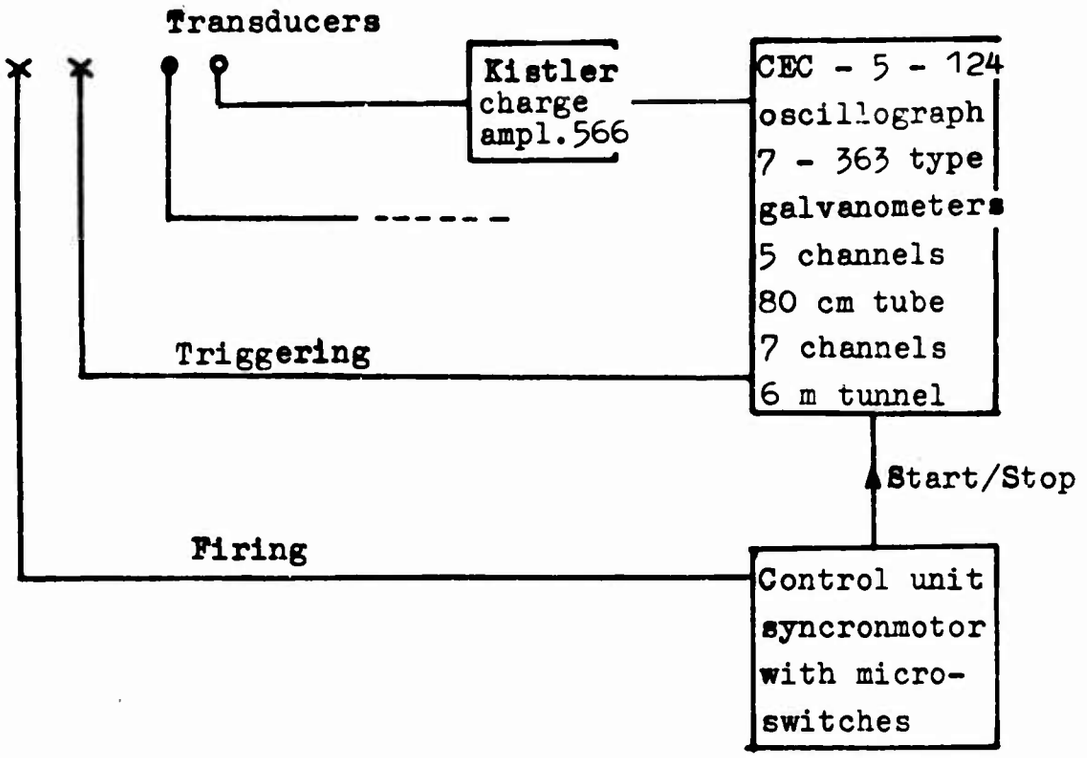

Fig III.9. Schematic electrical flow chart for 80 cm tube and 6 m diameter tunnel in rock tests

Typical records from oscilloscope and oscillograph is shown in the reproductions in fig III.10.

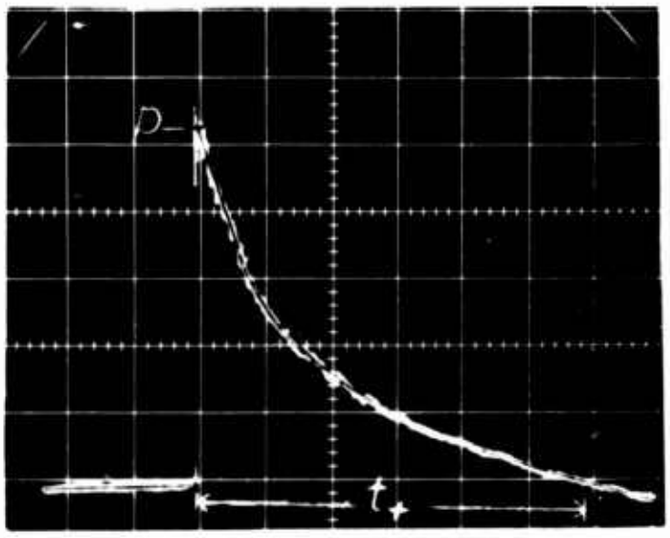

D = 5 cm, L = 1272 cm
Q = 9,5 g TNT
X = 1 ms/div, Y = 0,36 ato/div

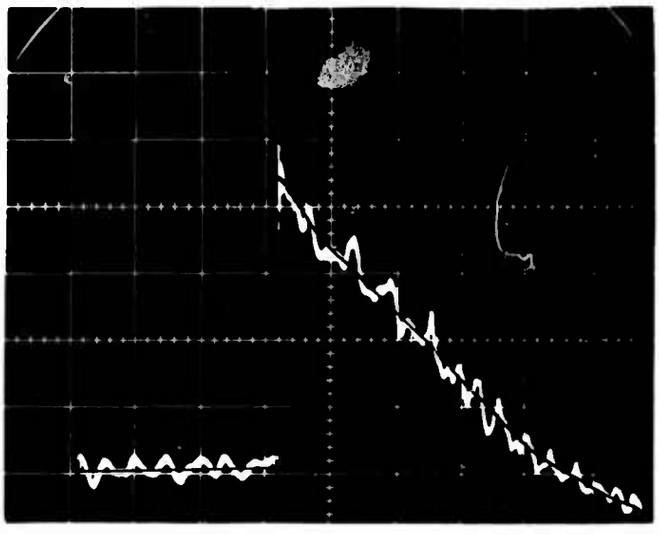

D = 20 cm, L = 587 cm
Q = 25,5 g TNT
X = 1 ms/div, Y = 0,67 ato/div

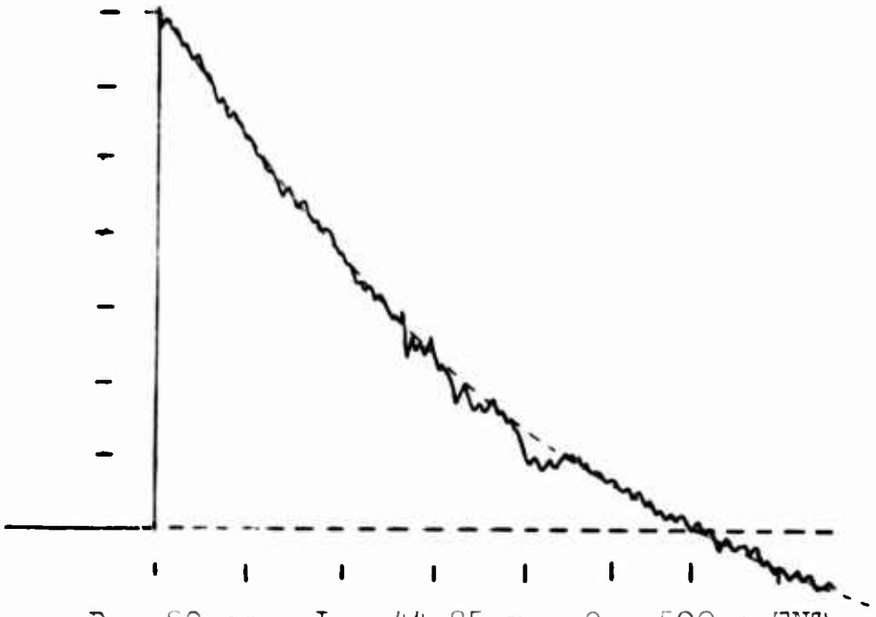

D = 80 cm, L = 44,85 m, Q = 500 g TNT
X = 100 ms/div, Y = 0,088 ato/div

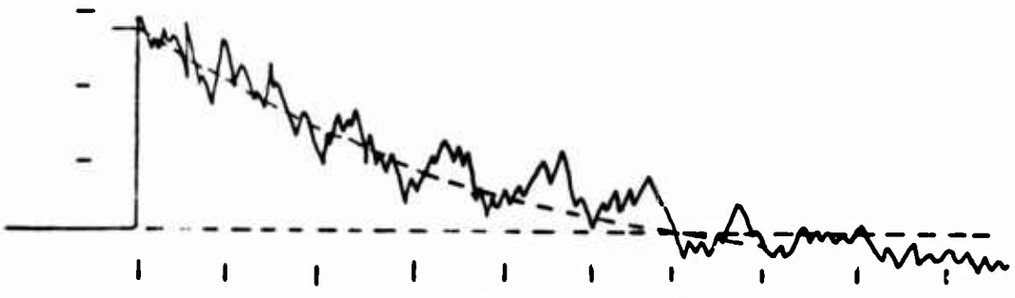

D = 6 m, L = 27 m, Q = 7 kg TNT
X = 100 ms/div, Y = 0,23 ato/div

Fig.III.10 Typical records from oscilloscope and oscillograph

III.7 Check of frontpressure with time of arrival measurements

As frontpressure is uniquely determined from tabulated blast velocity data, a simple check of frontpressure measurements from pressure-time records is possible by simple velocity measurements. This was done with the 5 cm diameter tube. 5 mm diameter holes were drilled through the wall with approximately 20 cm interval and selfmade folioswitches were taped over the holes and contact-time interval was recorded by a Hewlet-Packard counter. Comparison of the two methods is done in fig. III.11, and the difference is not more than expected from the time of arrival measurements.

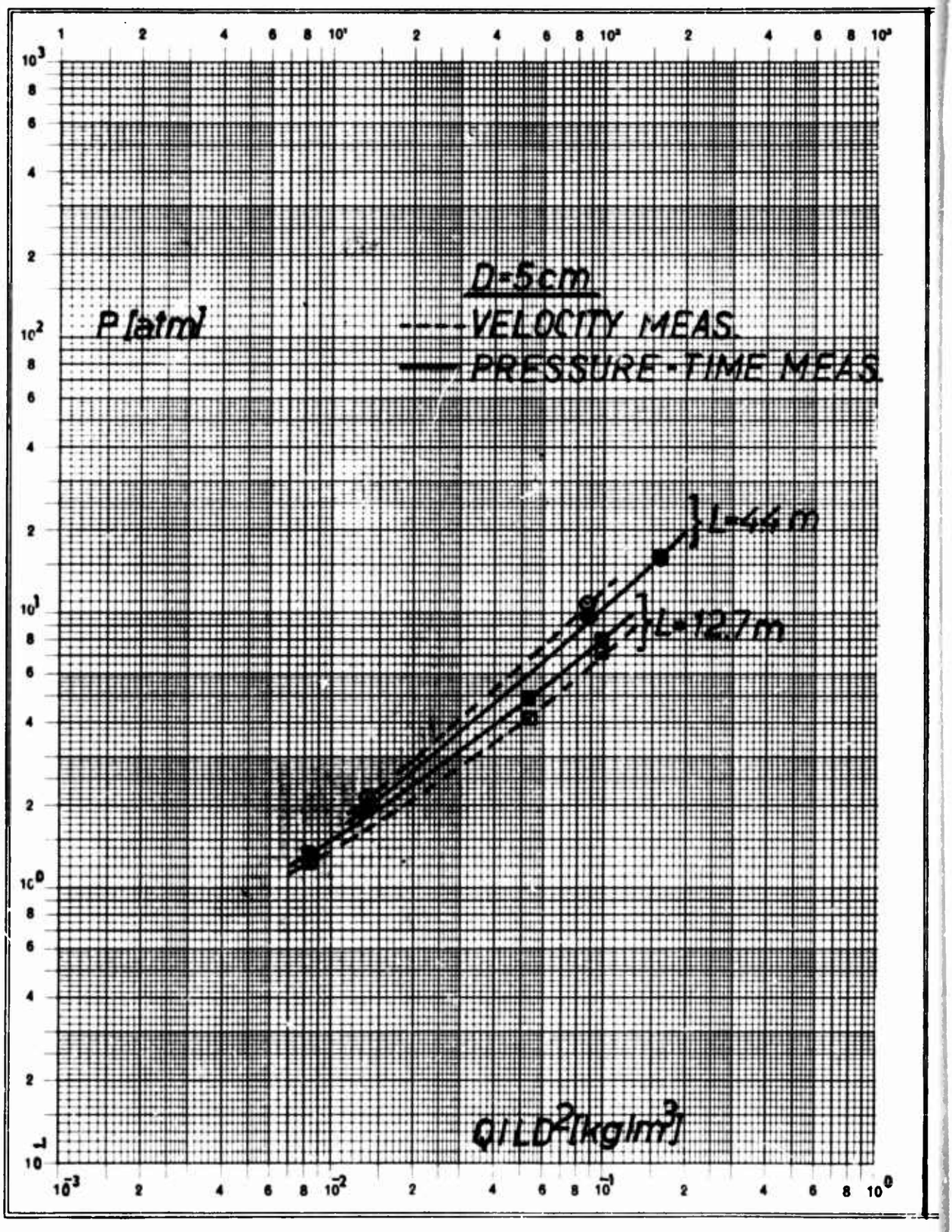

Fig.III.11 Comparison pressure-time measurements and velocity measurements in 5 cm tube

IV. P R E P A R A T I O N O F D A T A

IV.1 Interpretation of traces

As can be seen in fig III.10 the records posessed an irregular pressure-time trace, because of noise, irregularities in the blast wave because of non-ideal one-dimensional flow, overshoot in transducer, oscillograph etc. The records were then "averaged" by drawing a best fit smooth curve. However, the determination of pulse height by this method is estimated to give at least 5% uncertainty. For the determination of the impulse the uncertainty is even more, approx. 20% partly because the positive duration, t_+, is very uncertain. Definitions are given in fig IV.1.

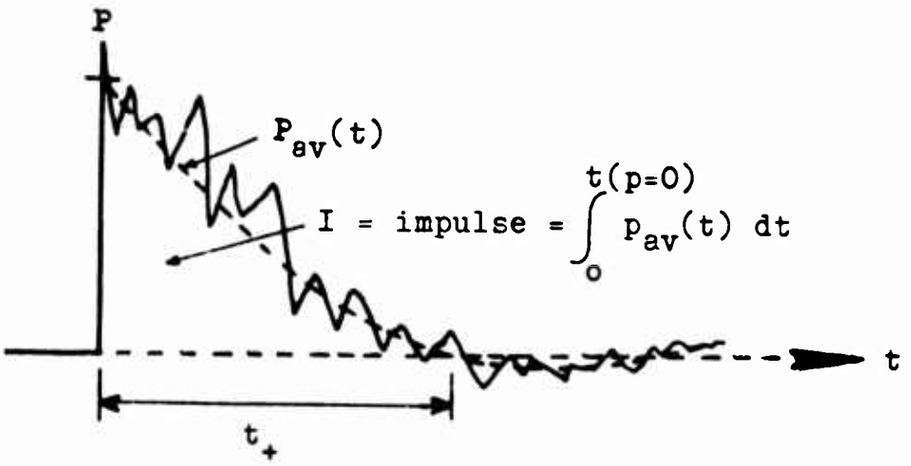

Fig IV.1. Definition of parameters

IV.2 Conversion of pictures to paper-tape

The method for conversion of the pressure-time traces to paper-tape is described in detail in ref /6/. The technique is quite simple and is shown schematically in fig. IV.2.

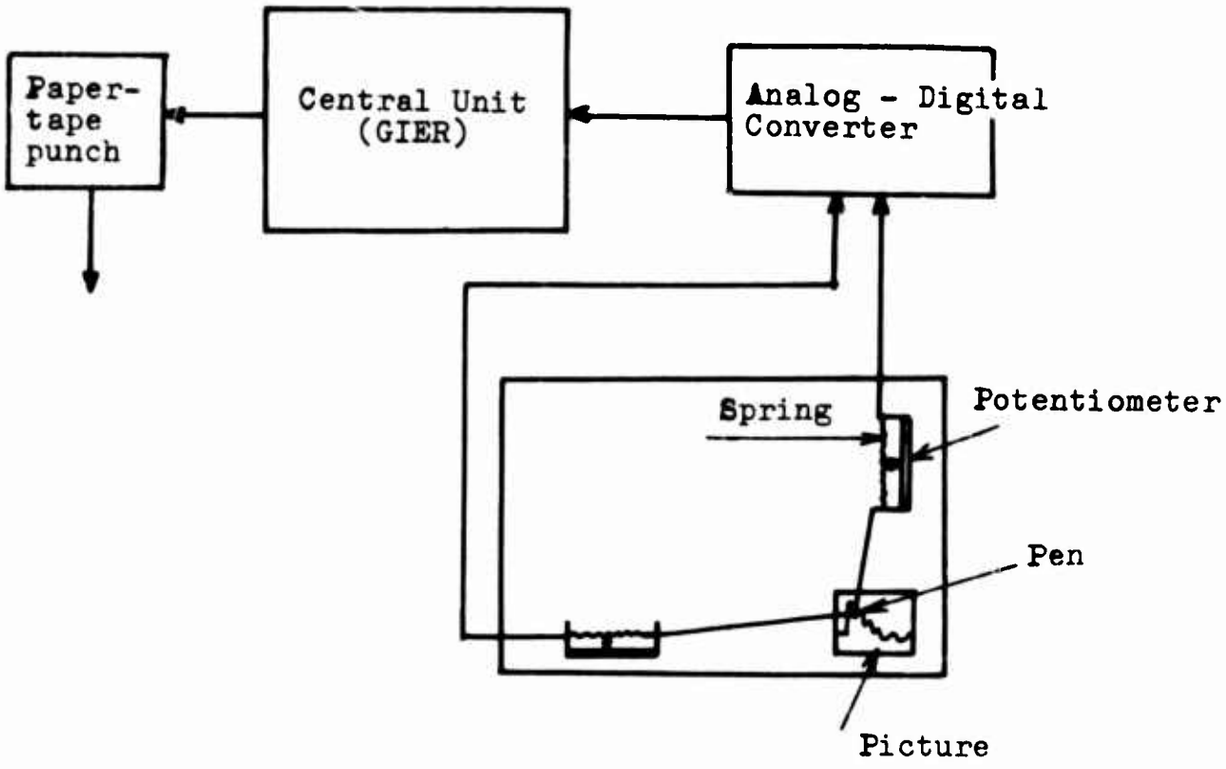

Fig IV.2. Schematic conversion of pictures to paper-tape

Two potentiometers give voltages which is a measure of the x- and y-coordinates of a sufficient chosen number of discrete points on the averaged trace (typical 20 points were chosen).

IV.3 Computer work

The further modification of converted data, main programs etc. are too lengthy to be described in detail here, but some features will be mentioned. The computing was done with an UNIVAC 1107.

The frontpressure P was picked out as the largest ordinate.

The impulse of positive pressure front:

$$I = \int_{0}^{t_+(p=0)} p_{av}\,(t) \cdot dt$$

was computed with common trapezoid-integration.

t_+ was found as time from pressurefront to averaged pressure curve again reaches zero.

V. RESULTS AND DISCUSSION

V.1 Frontpressure

Fig V.1 to V.5 presents the data relating the observed front overpressure p to tube/tunnel position in L/D units with TNT charge weight as parameter.

From this is it clear that for the same tube, the higher the peak pressure, the greater the blast-wave attenuation.

At longer L/D distances the results demonstrate that the attenuation is described roughly by

$$p = C(p_o)(L/D)^{k_1(p_o)} \qquad (V.1)$$

Taking the initial pressure p_o at L/D=20, we may find the constants $k(p_{20})$ from the averaged curves in fig V.5, (by extrapolating straight lines backwards to L/D=20 for the 5 cm tube).

This is shown in fig V.6. For $p_{20} \gtrsim 1$ atm the functional dependence of k_1 is described by

$$k_1 \simeq -0{,}433 \log p_{20} - 0{,}653 \qquad (V.2)$$

and

$$C \simeq 6{,}79 \cdot p_{20}^{1{,}61} \qquad (V.3)$$

hence

$$p = 6{,}79\, p_{20}^{1{,}61} \left(\frac{L}{D}\right)^{-0{,}433 \log p_{20} - 0{,}653} \qquad (V.4)$$

This is shown in fig V.6 and V.7 to be rough approximations for the 5, 20 and 80 cm diameter tubes for p_{20} in the region 1 to 200 atm (extrapolated back from "long range attenuation" whereas for the attenuation tunnel in rock and $p_{20} \lesssim 1$ atm for the 80 cm diameter tube we do not have this simple functional dependence.

The exponent k seems to reach a more or less constant value for $p_{20} \lesssim 0{,}5$ atm.

As stated before, it is evident that attenuation is a function of the relative wall roughness, i.e. dependent on the parameter $\frac{e}{D}$. Within the experimental uncertainty one would not expect significant difference in attenuation for the steeltubes and the concrete tube. ($\frac{e}{D}$ between 0,03% and 0,5%). This is confirmed in fig V.6. The tunnel in rock with roughness $\frac{e}{D} \simeq 8\%$ seem to give more attenuation in the pressure region of overlapping, i.e. $p_{20} \simeq 0,1 - 1$ atm.

Additional experiments with systematic change of roughness in one tube and comparison of different tubes with varying diameter are hoped to be the next step in our series of experiments.

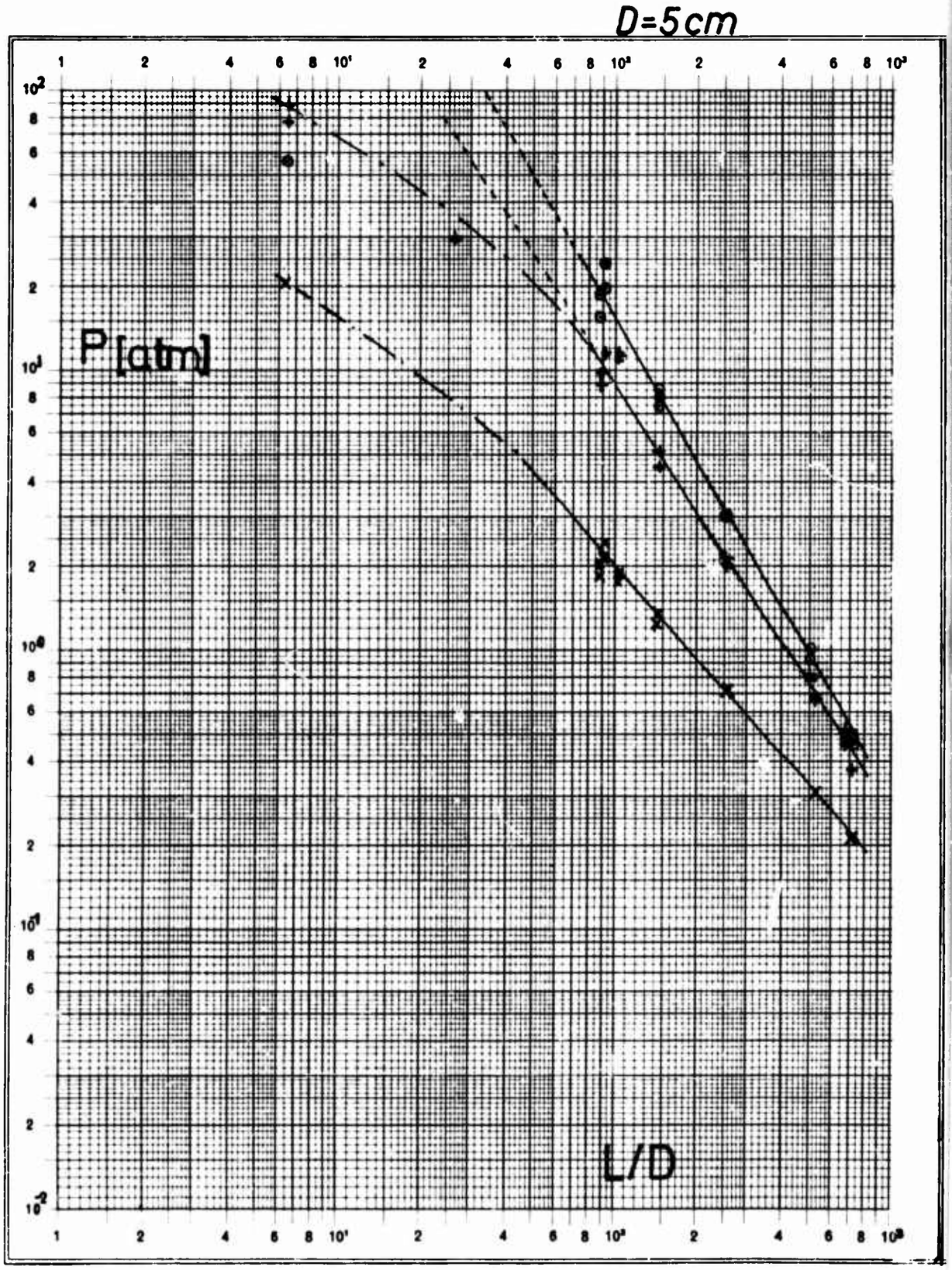

Fig.V.1 Frontpressure versus tube position in L/D units in 5 cm tube

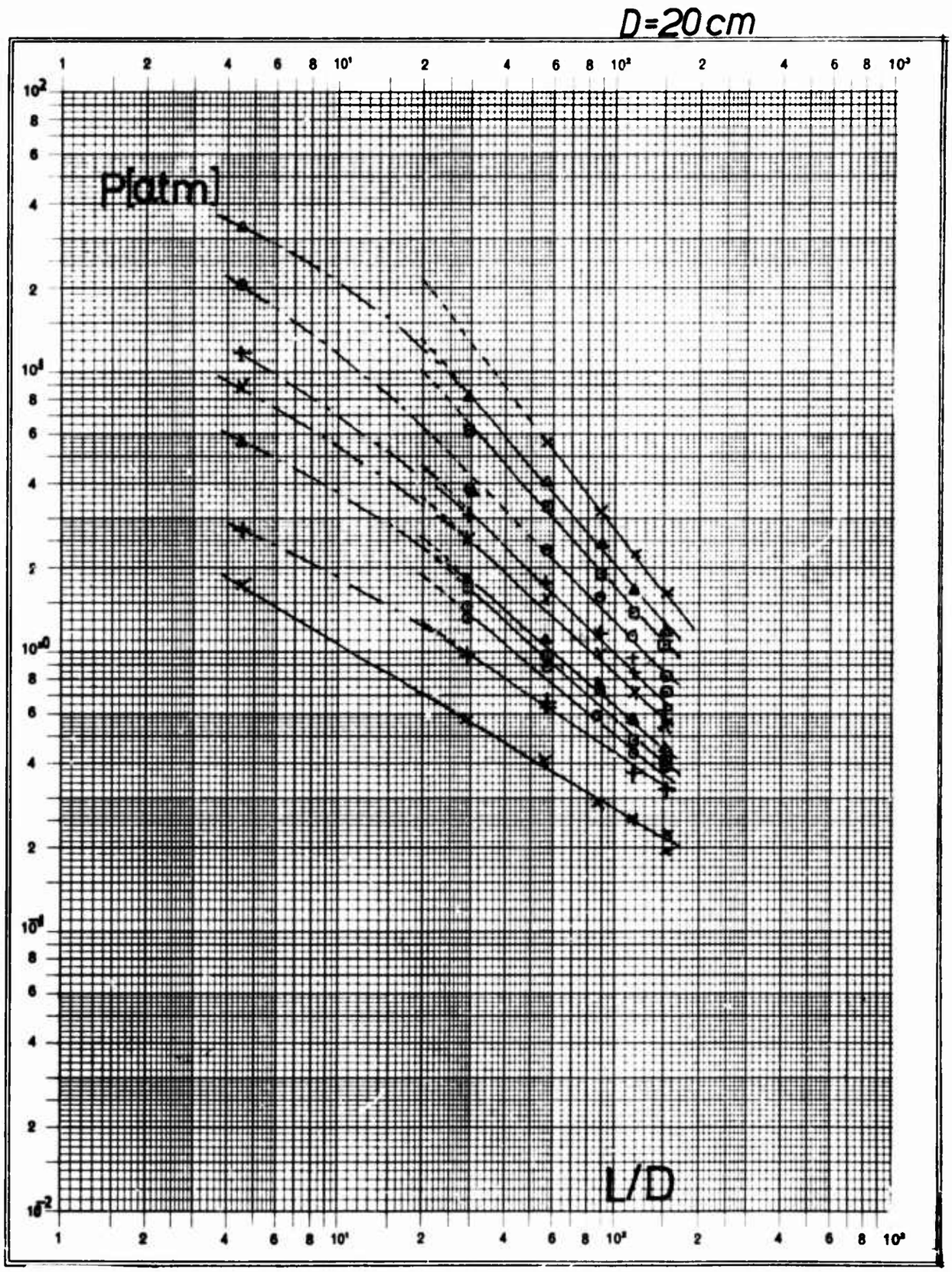

Fig.V.2 Frontpressure versus tube position in L/D units in 20 cm tube

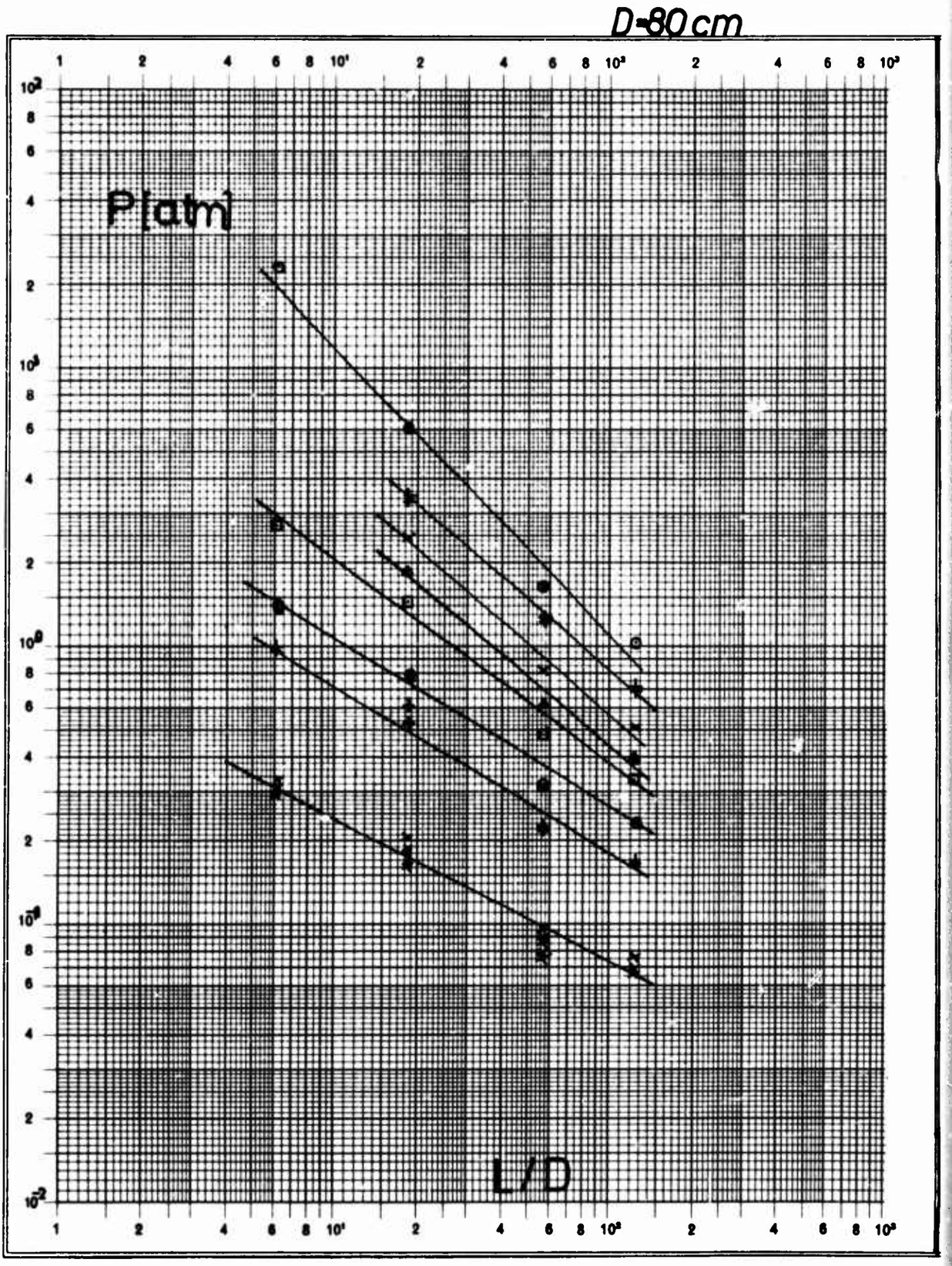

Fig.V.3 Frontpressure versus tube position in L/D units in 80 cm tube

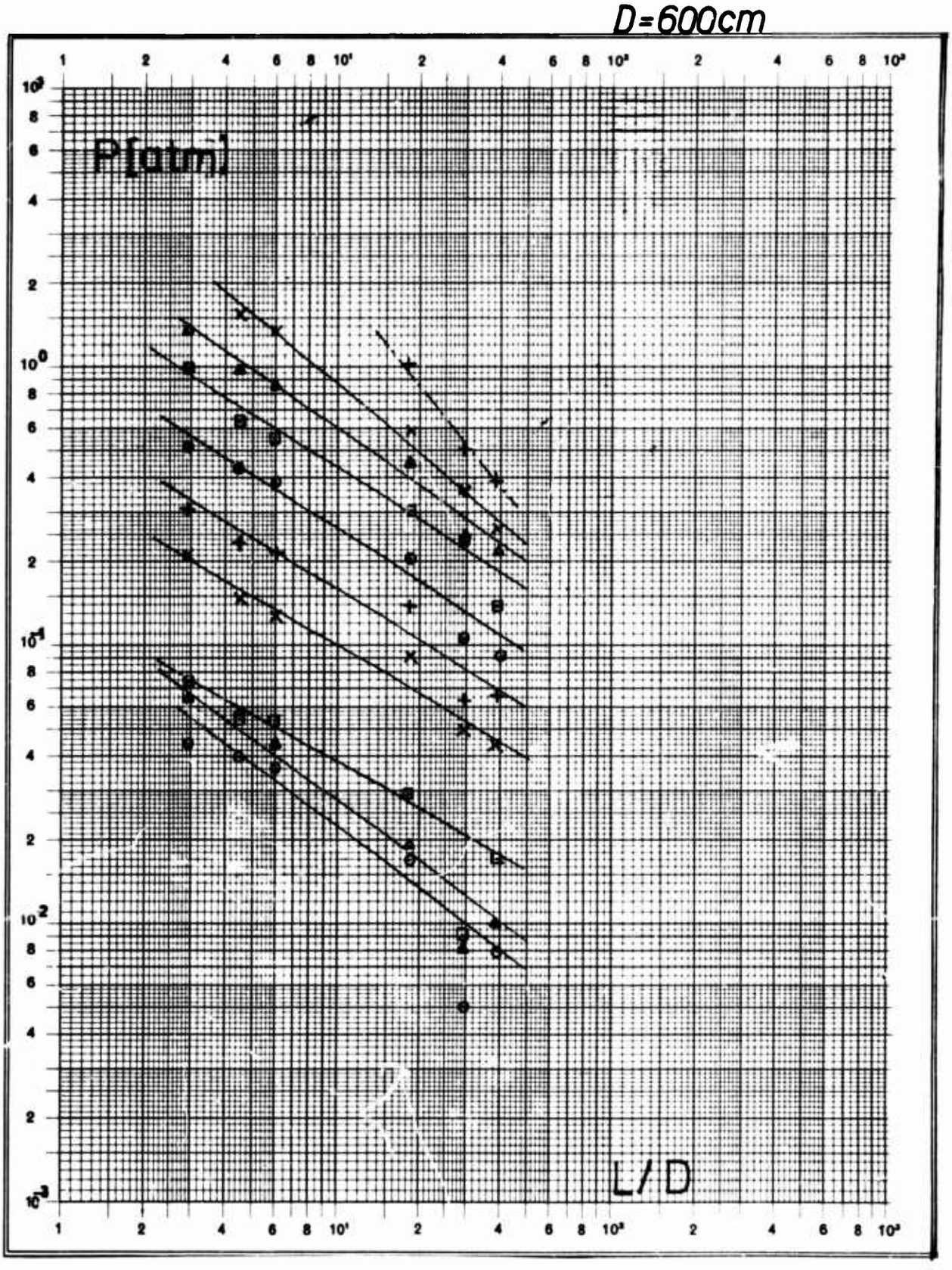

Fig.V.4 Frontpressure versus tunnel position in L/D units in 6 m tunnel in rock

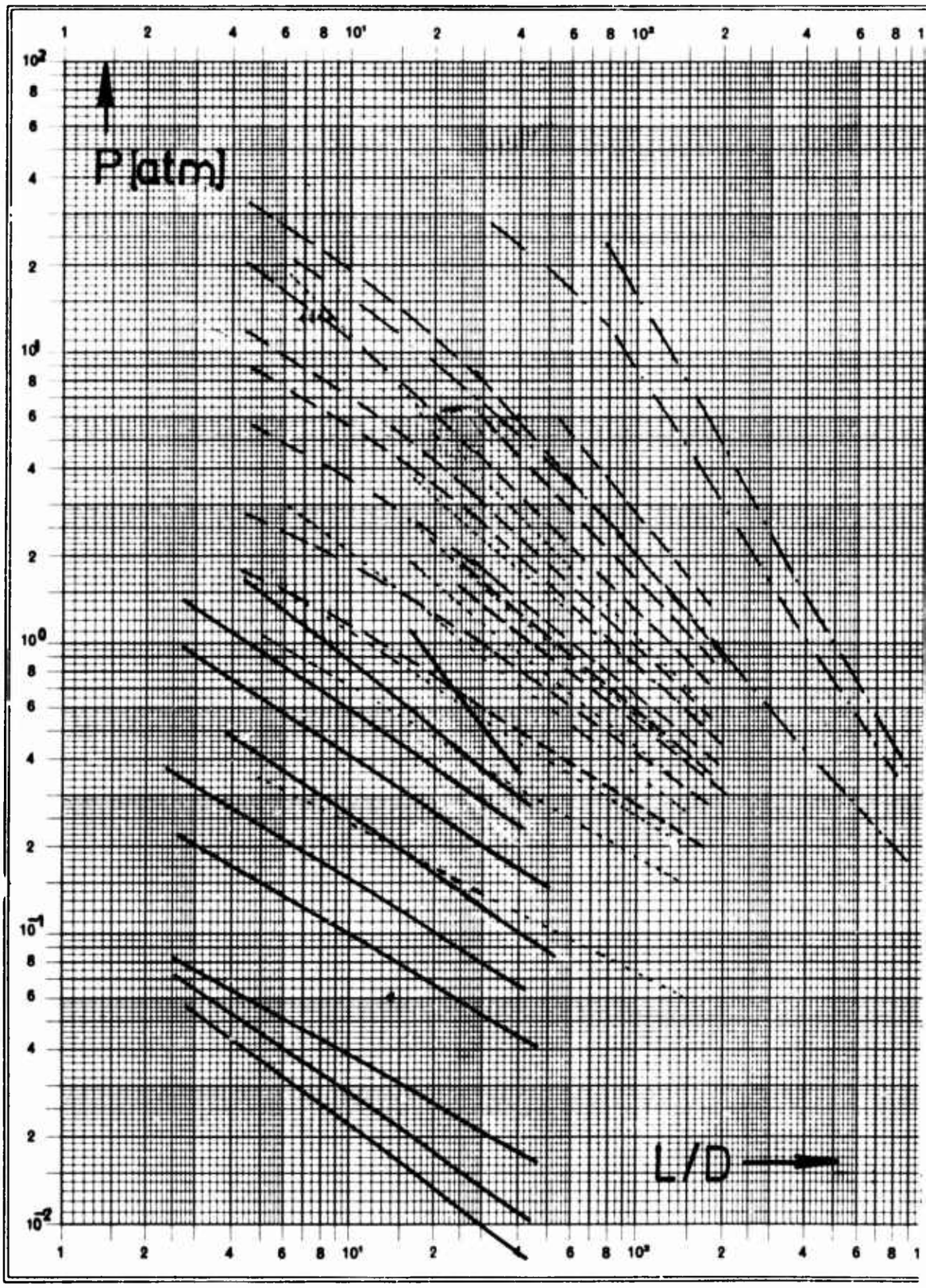

Fig.V.5
Comparison of frontpressure attenuation for different tubes and tunnel in rock

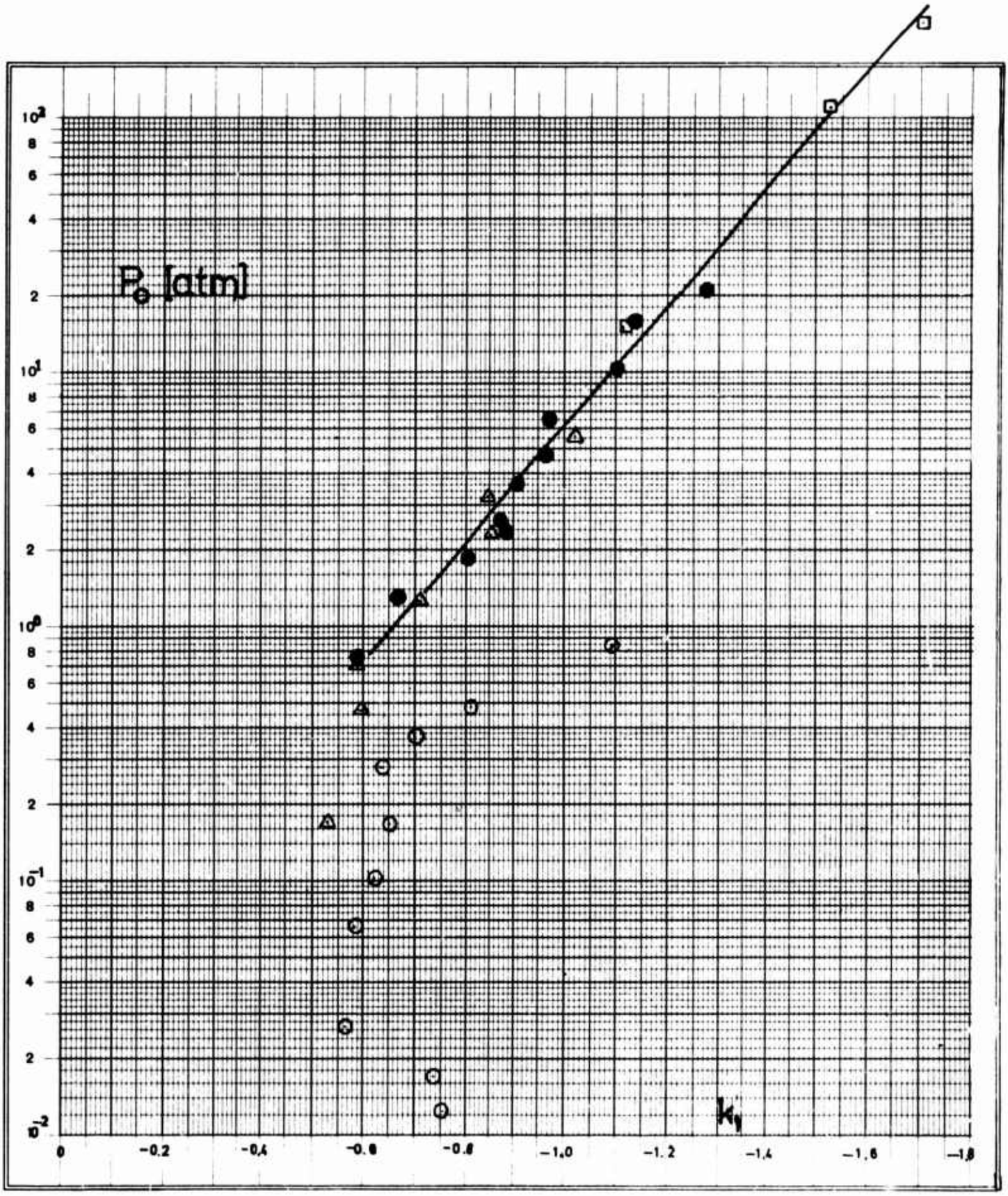

□ D = 5cm
● 20
▲ 80
⊙ 600

Fig.V.6 Attenuation constant k_1 for longrange attenuation versus initial frontpressure p_{20} at L/D = 20 from figures V.1 to V.5

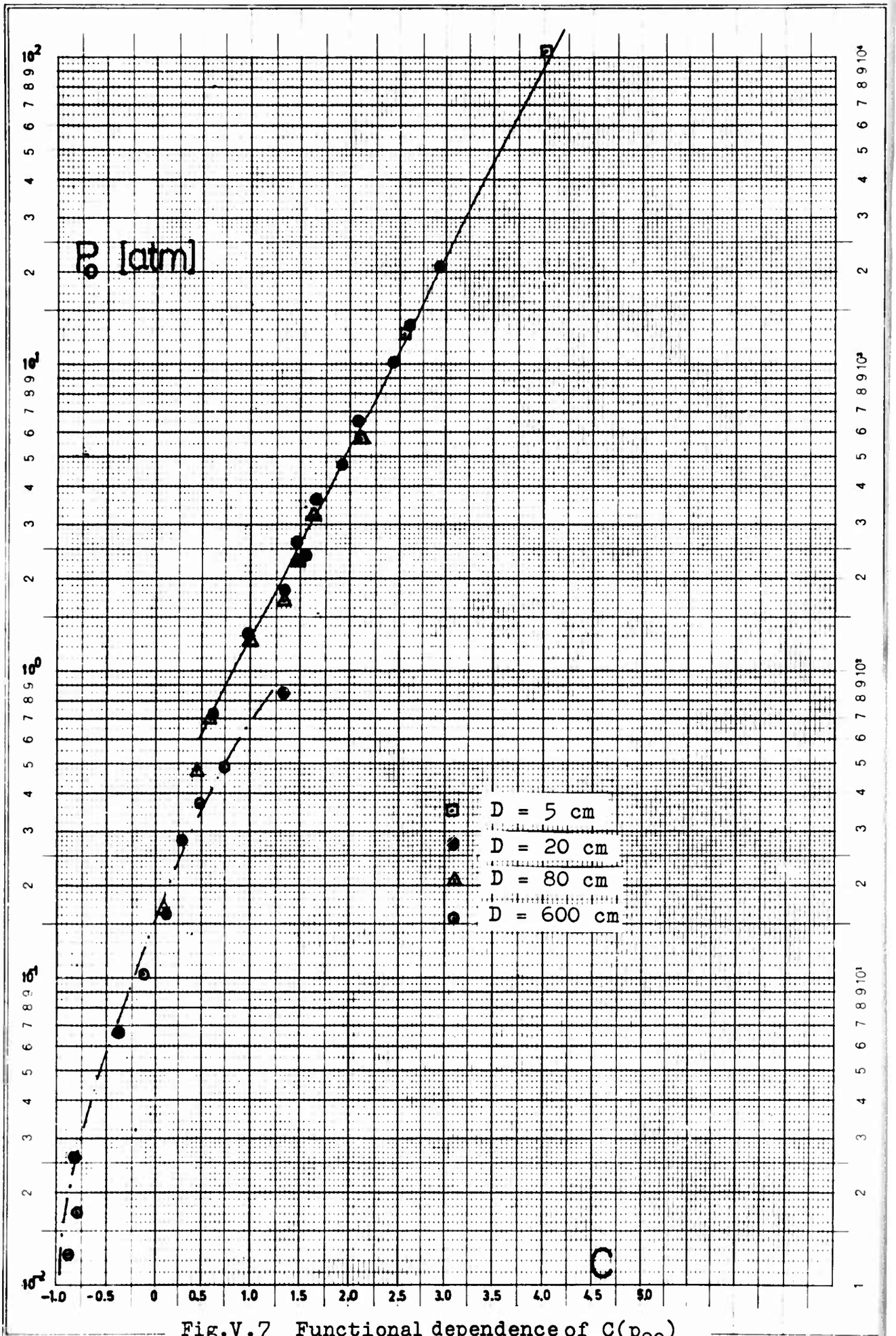

Fig.V.7 Functional dependence of $C(p_{20})$ in eq. $p = C(p_{20})\, L/D^{k(p_{20})}$

Checking of the validity of the scaling law proposed in chapter II.2 eq (II.9) for the front pressure

(II.9) $$p = f\left(\frac{Q}{LD^2}\right) = f(Q_E)$$

is shown in figures V.8 to V.12.

The 5 cm tube results in fig V.8, 20 cm in fig V.9, 80 cm in fig V.10 and the 6 m tunnel in rock in fig V.11. The influence of the wall attenuation clearly manifests itself in the lowering of the pressure curves with increasing L/D values. Direct comparison of all data is given in fig V.12.

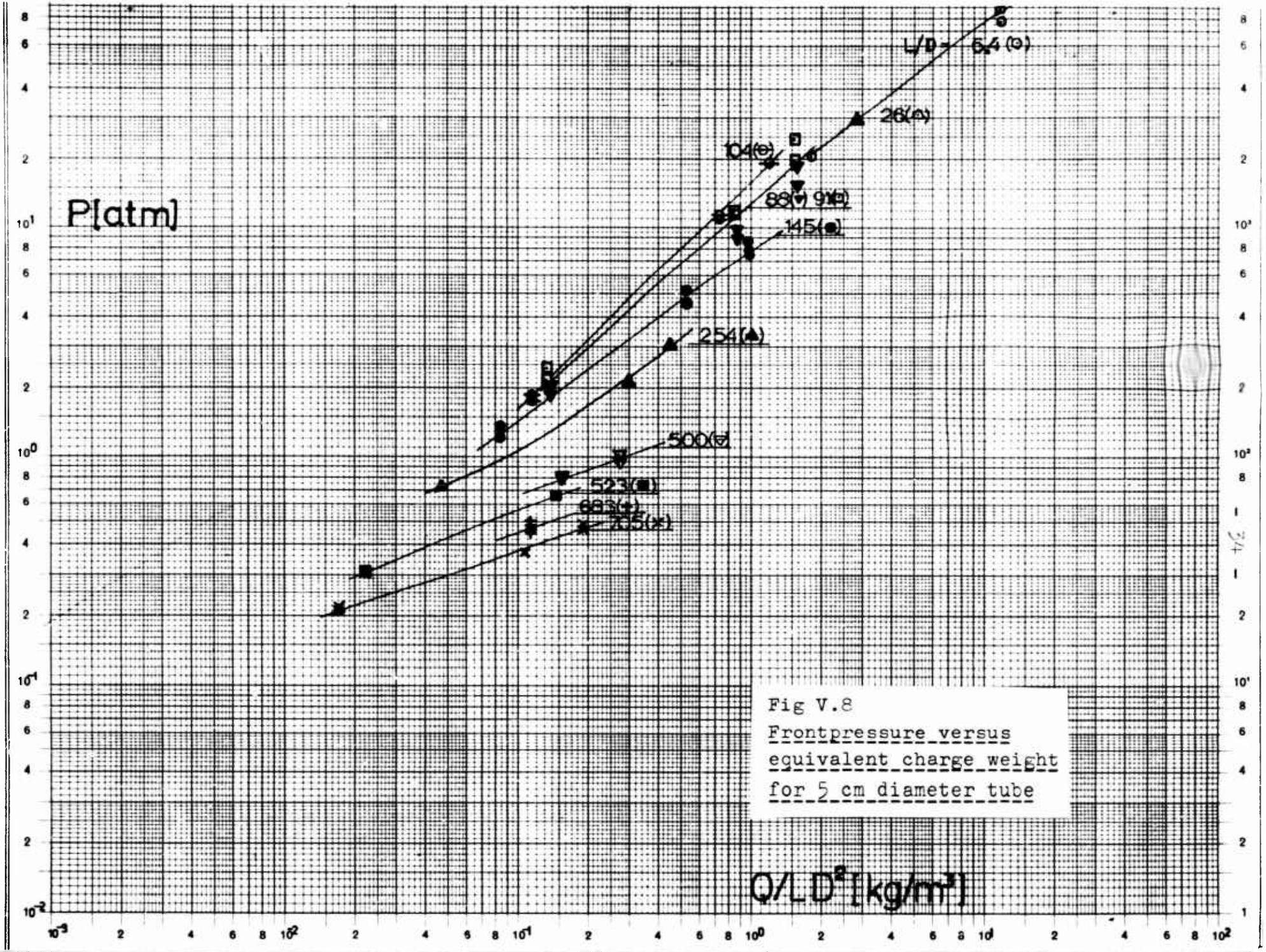

Fig V.8
Frontpressure versus equivalent charge weight for 5 cm diameter tube

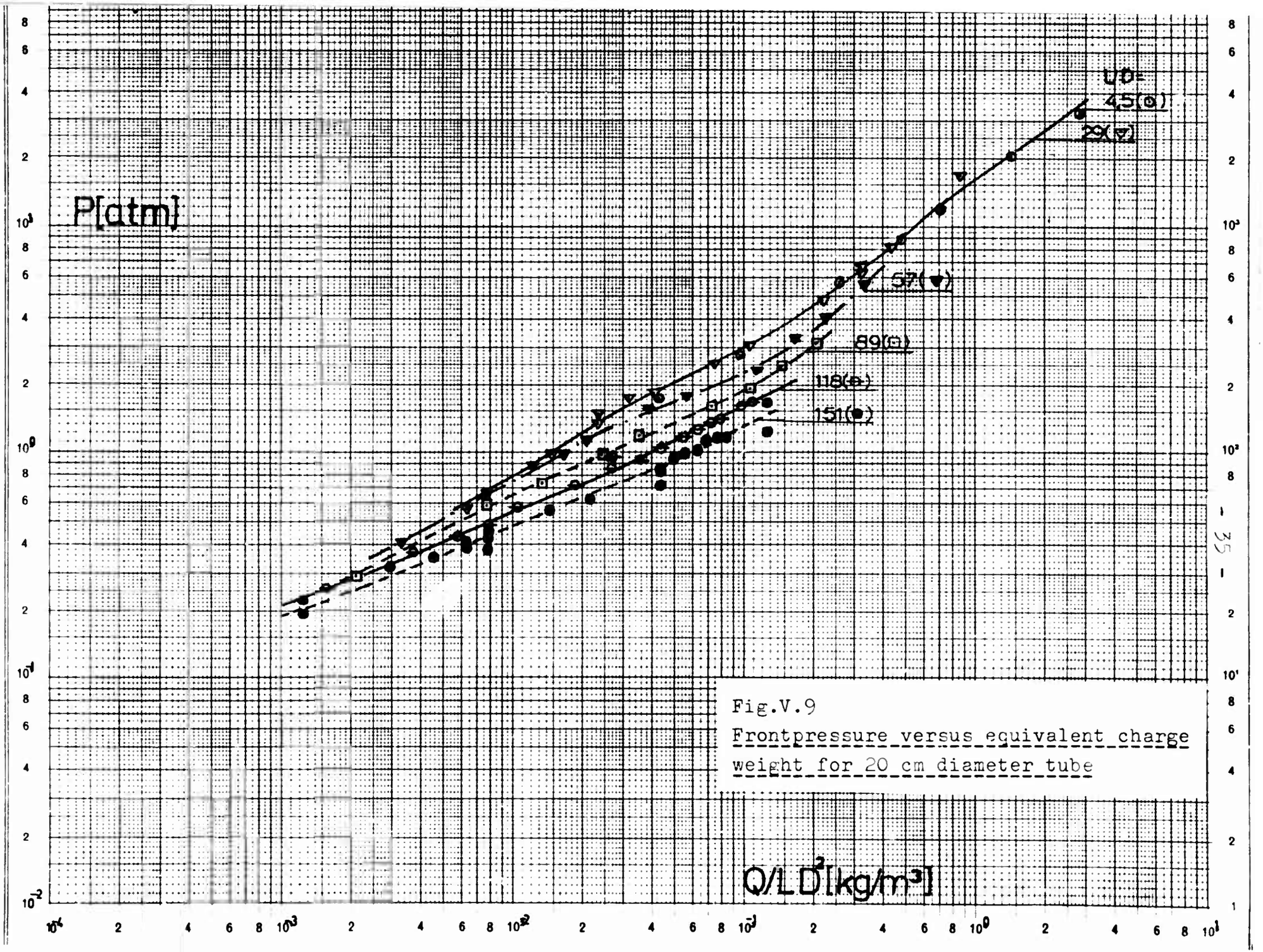

Fig.V.9
Frontpressure versus equivalent charge weight for 20 cm diameter tube

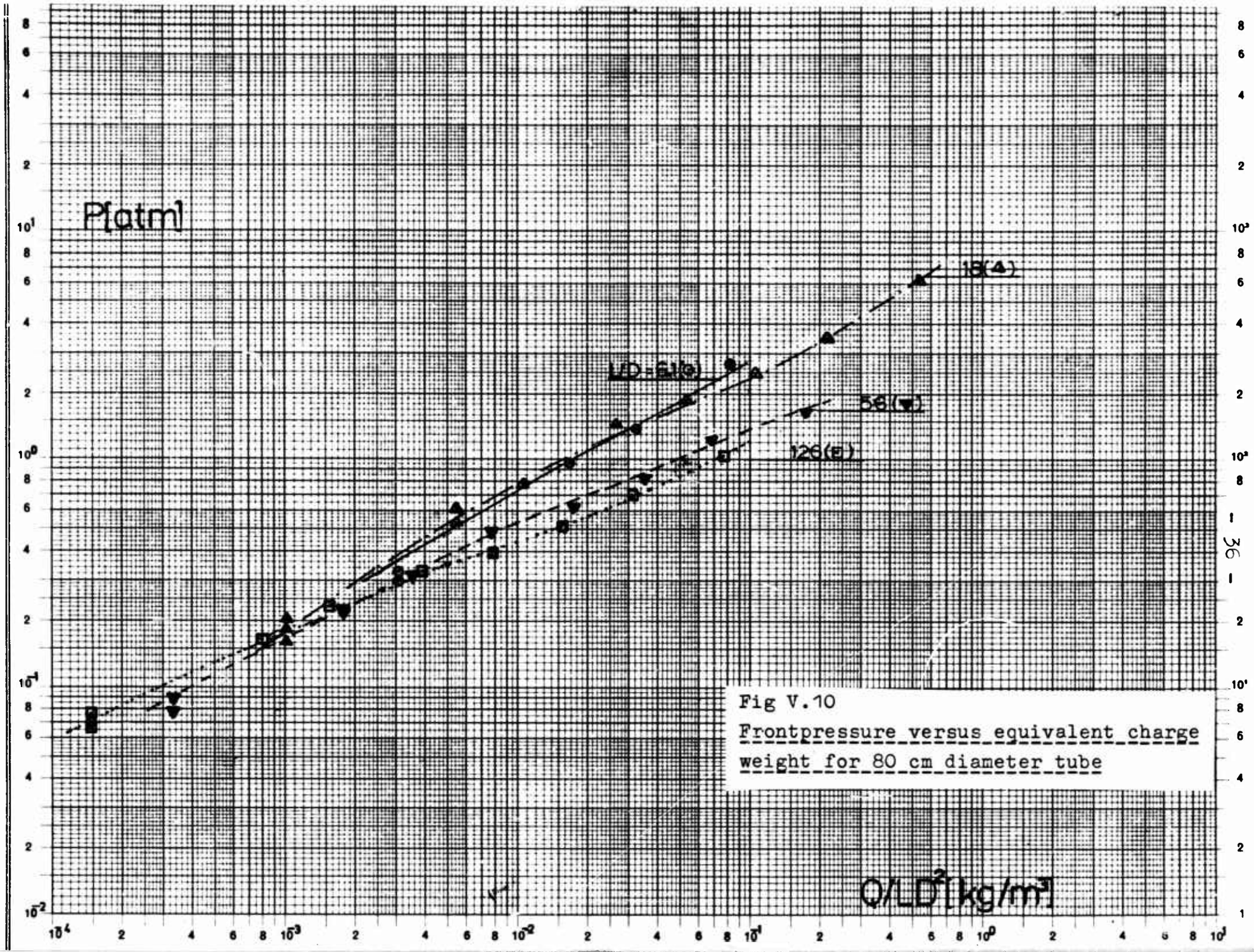

Fig V.10
Frontpressure versus equivalent charge weight for 80 cm diameter tube

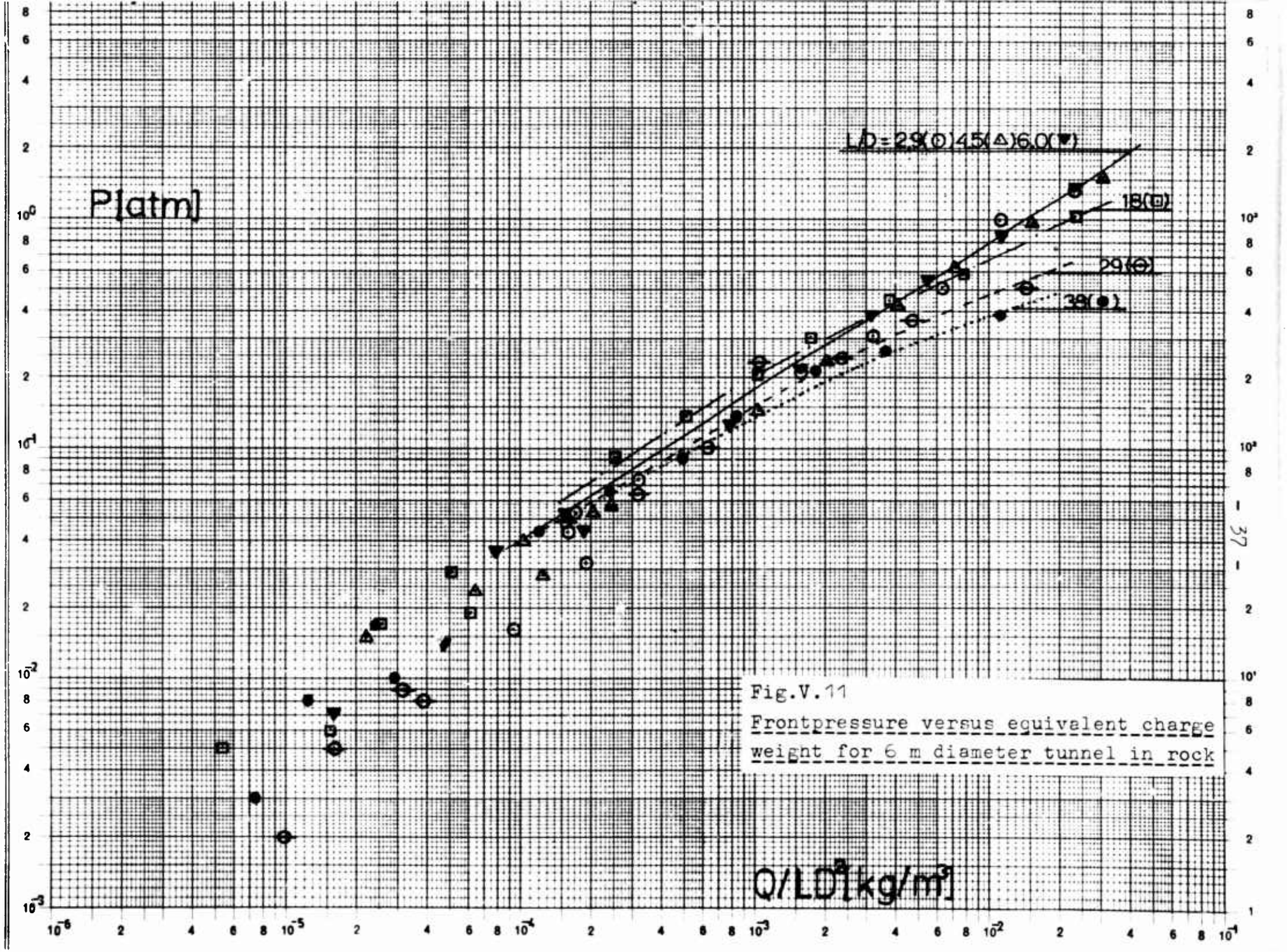

Fig.V.11
Frontpressure versus equivalent charge weight for 6 m diameter tunnel in rock

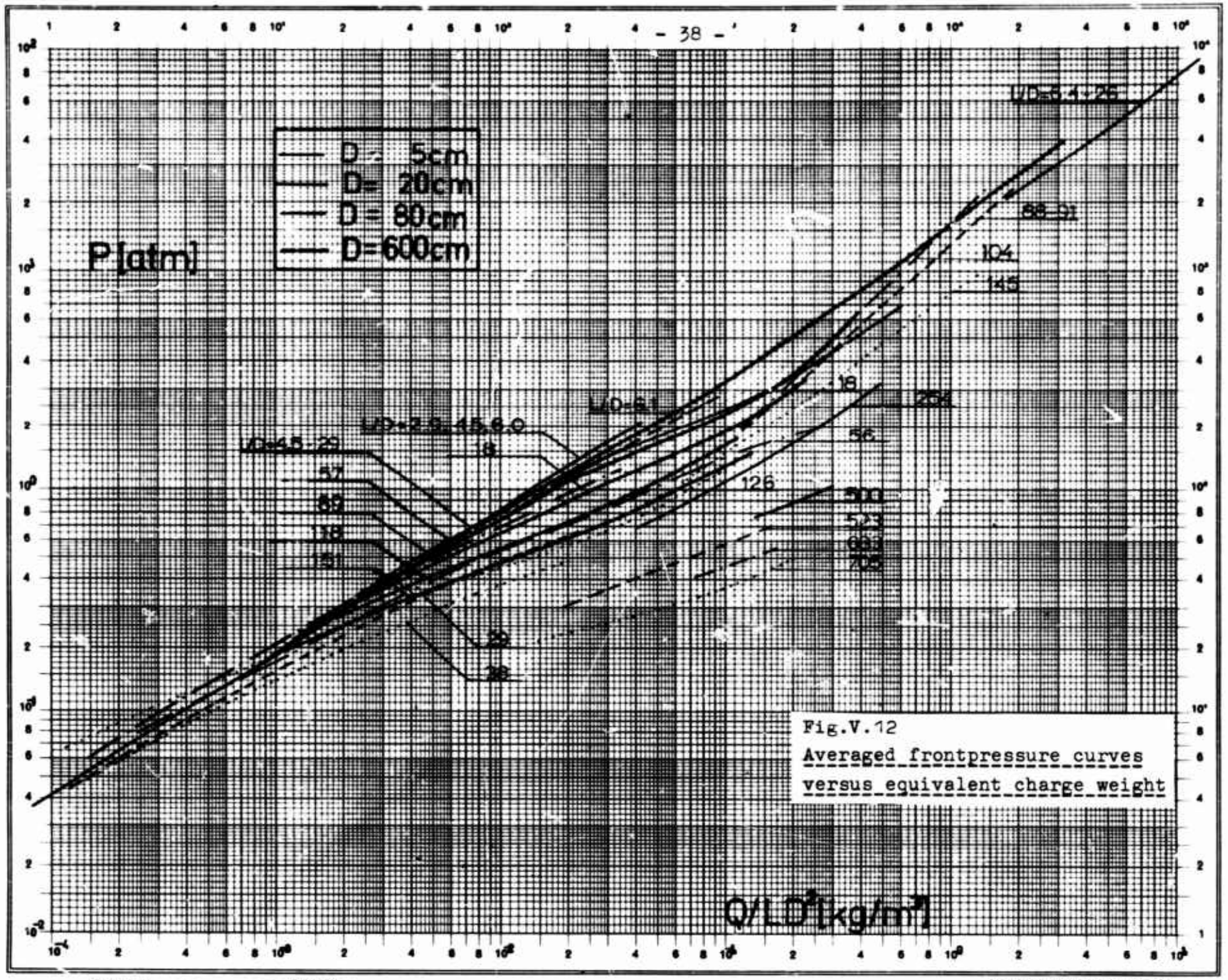

Fig.V.12
Averaged frontpressure curves versus equivalent charge weight

The overall feature is that the deviation from the ideally expected scaled smooth frontpressure curve is greater, the smaller the tube cross section.

Plotting the pressure versus L/D with Q_E as parameter we may extrapolate to $L/D \rightarrow 0$ and get the "unattenuated" scaled pressure curve, $p_{so}(Q_E)$.

The average L/D influence on the attenuation is evaluated to have exponential behaviour as

(V.6) $p = p_{so} \exp(-k \cdot (L/D))$

The damping constant k depends on p_{so} and tube/tunnel and is expressed as the fractional loss in frontpressure per diameter of travel, i.e., as

(V.7) $-D(dp/dx)/p = k$

This constant is estimated in fig V.13.

The tunnel shows considerably greater wall attenuation than the smoother tubes.

Emerich et al. in ref /4/ gives a value $k = (1,4 \pm 0,8) \cdot 10^{-3}$ as a mean value, for a 3,5 and 15,3 cm diameter tube with p_{so} between 0,1 and 1 atm, which roughly lies in the region of our estimations.

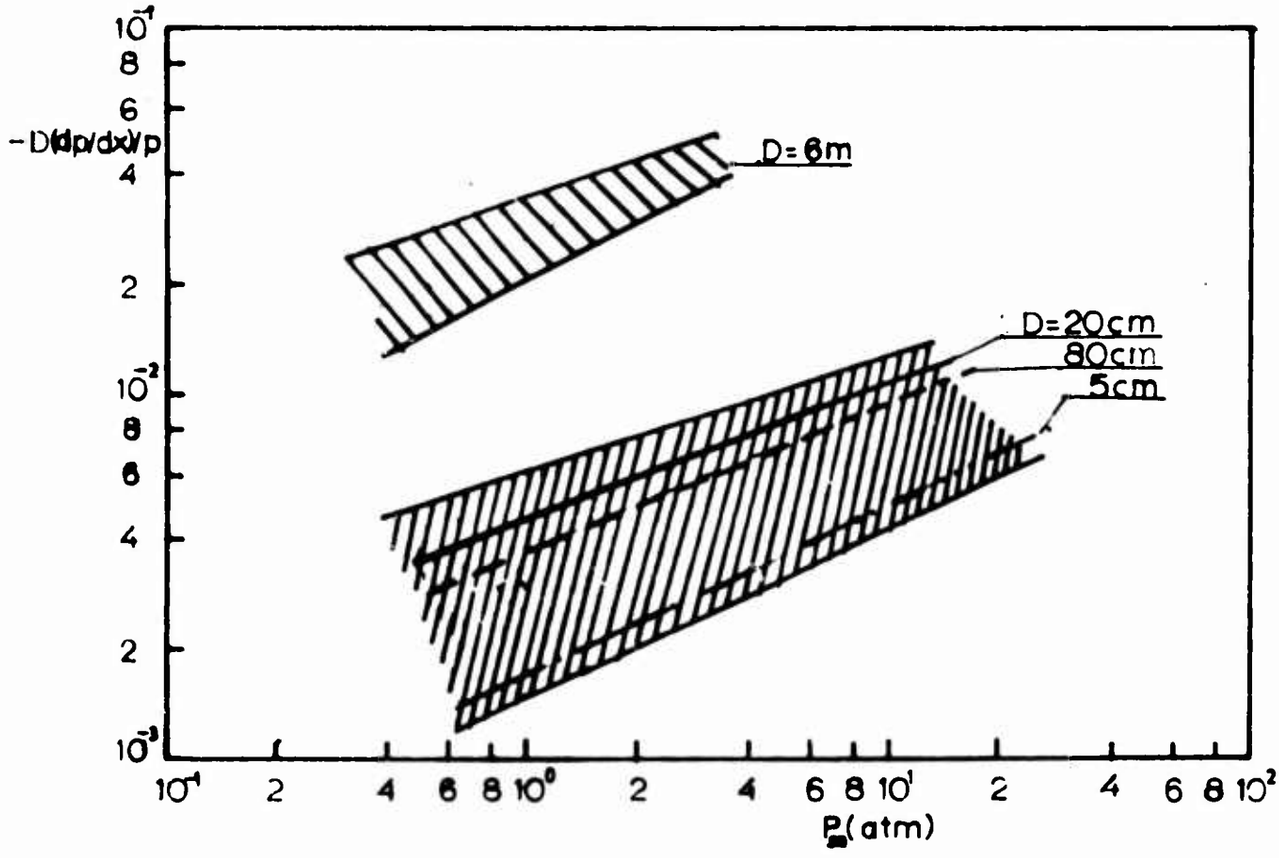

Fig V.13 Fractional changes in pressure from scaled unattenuated curve per unit distance of travel in tube diameters

Comparative tests done by Norwegian Defence Research Establishment /5/ in a tunnel in rock of effective diameter 4,8 ± 0,5 m, i.e. roughness about 13% with charges ranging from 10 to 500 kg TNT and L/D = 1,9 - 12, shows good agreement with our experiments.

V.2 Impulse

The scaling law proposed in chapter II.2 eq. (II.10) for the impulse I

(II.10) $$\frac{I \cdot D^2}{Q} = g\left(\frac{Q}{LD^2}\right) = g(Q_E)$$

($\frac{I \cdot D^2}{Q}$ hereafter called reduced impulse)

is checked with experiments in fig V.14 - V.18. The data here are considerably fewer than for the pressure which is because rarefaction waves from the open end of the tubes sometimes destroyed the correct pressure time history.

Direct comparison at comparable distances in L/D units in fig V.17 and V.18 shows a significant lower reduced impulse for the tunnel in rock at large L/D ($\simeq 38$) compared with the tubes.

We may use the same procedure as described in V.1 for the pressure letting $L/D \rightarrow 0$ and find the "unattenuated" scaled impulse curve. For $L/D \lesssim 7$ the attenuation is not significantly different for the tubes and tunnel in rock.

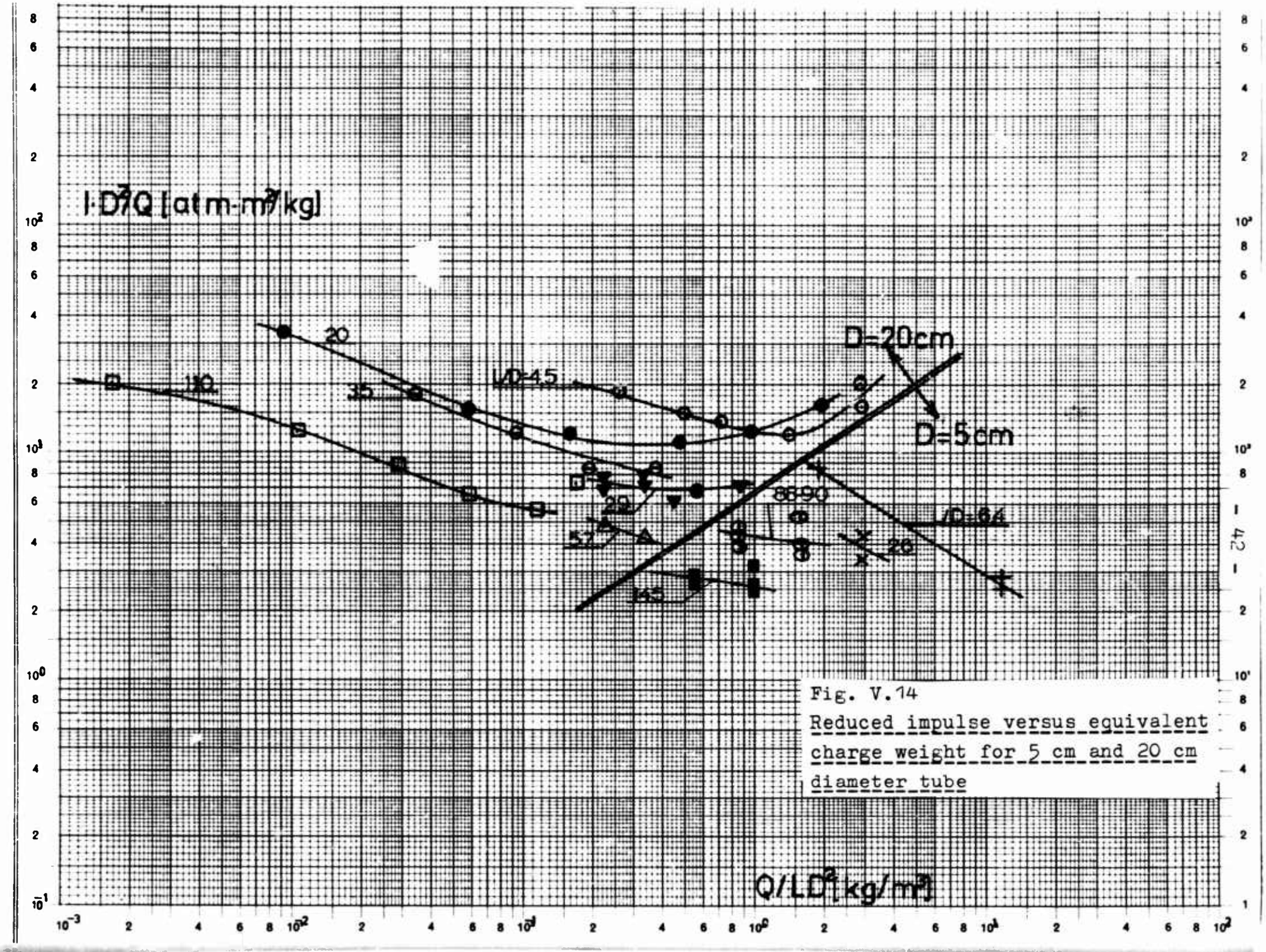

Fig. V.14

Reduced impulse versus equivalent charge weight for 5 cm and 20 cm diameter tube

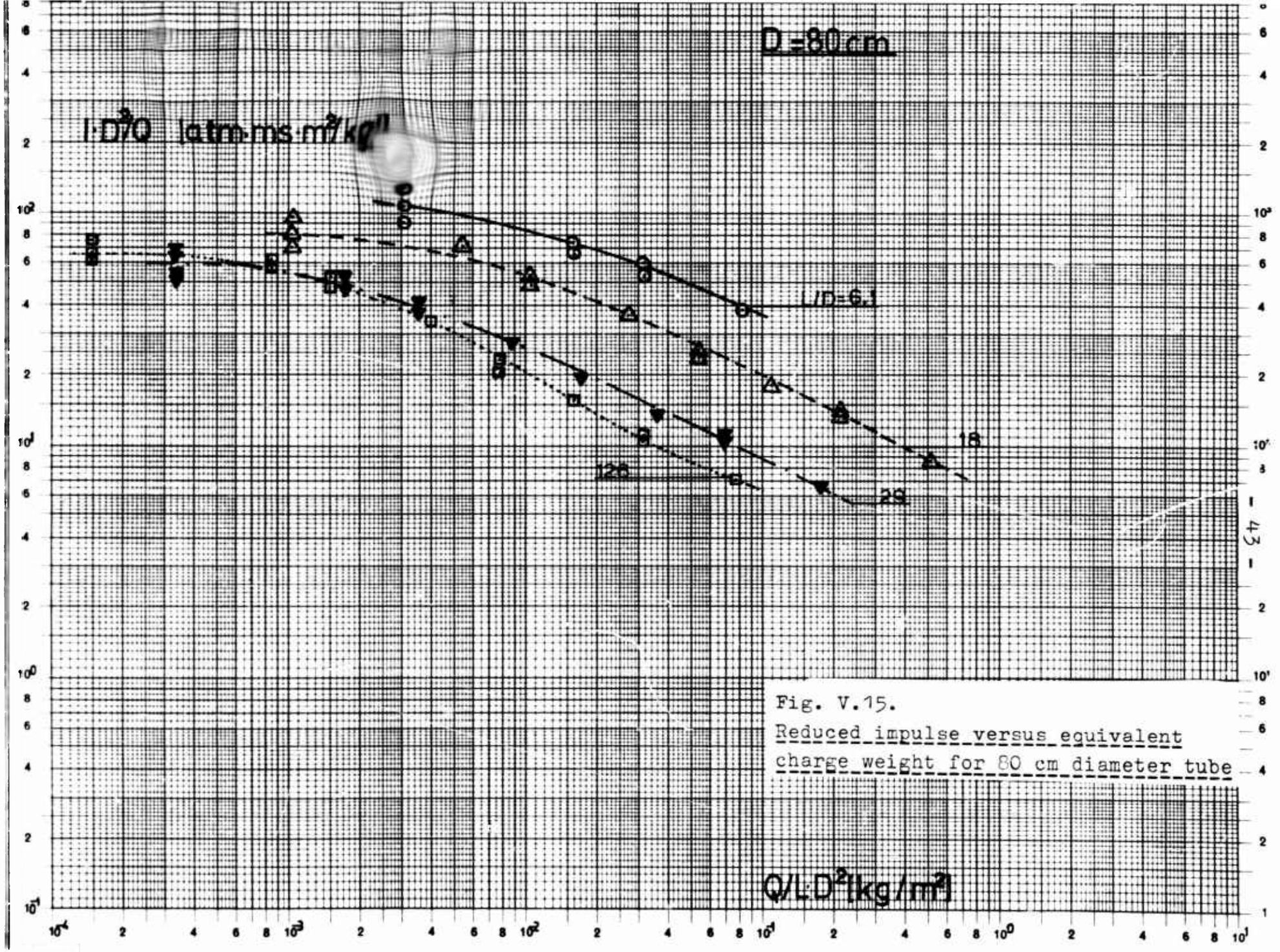

Fig. V.15.
Reduced impulse versus equivalent charge weight for 80 cm diameter tube

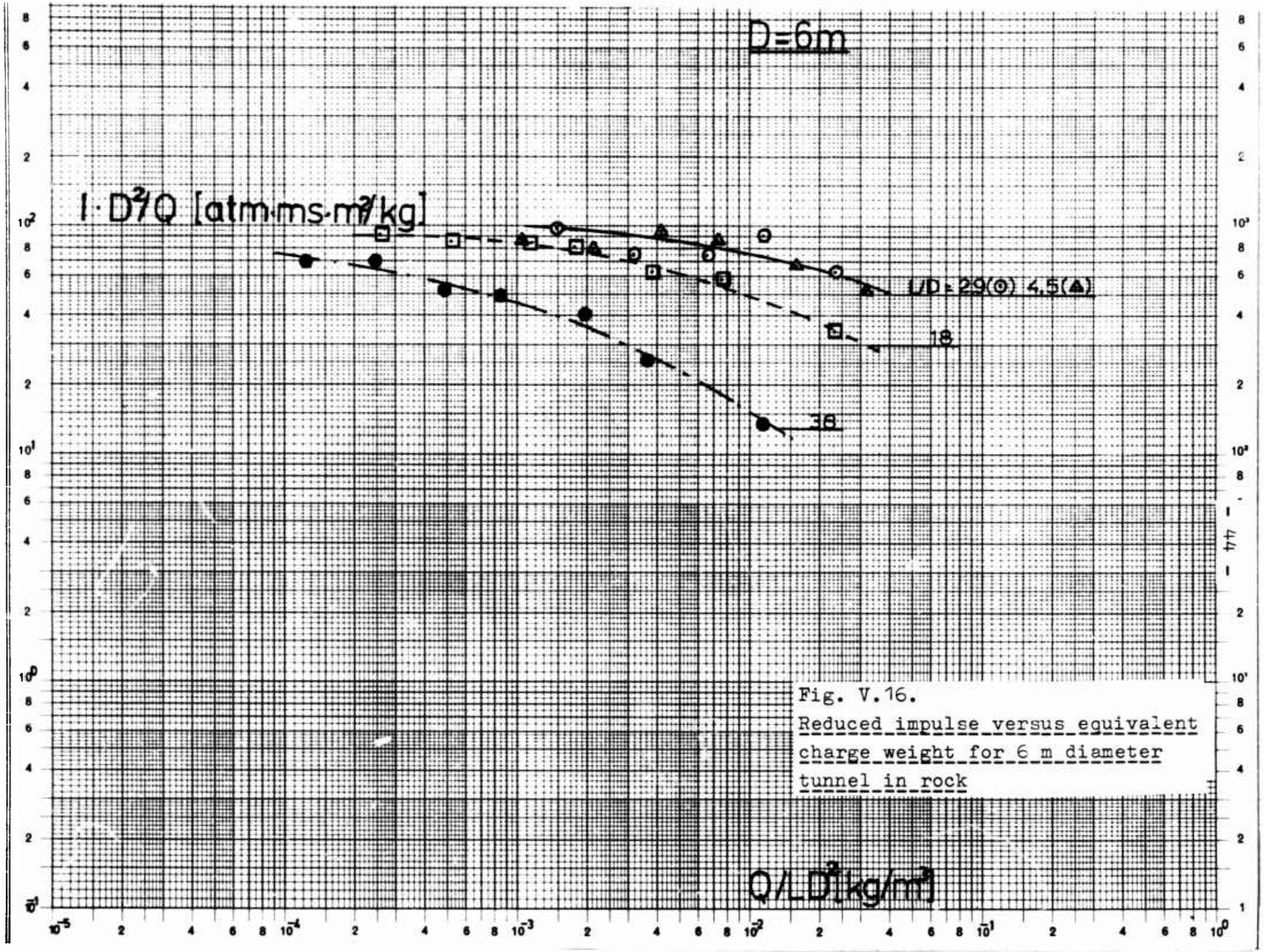

Fig. V.16.
Reduced impulse versus equivalent charge weight for 6 m diameter tunnel in rock

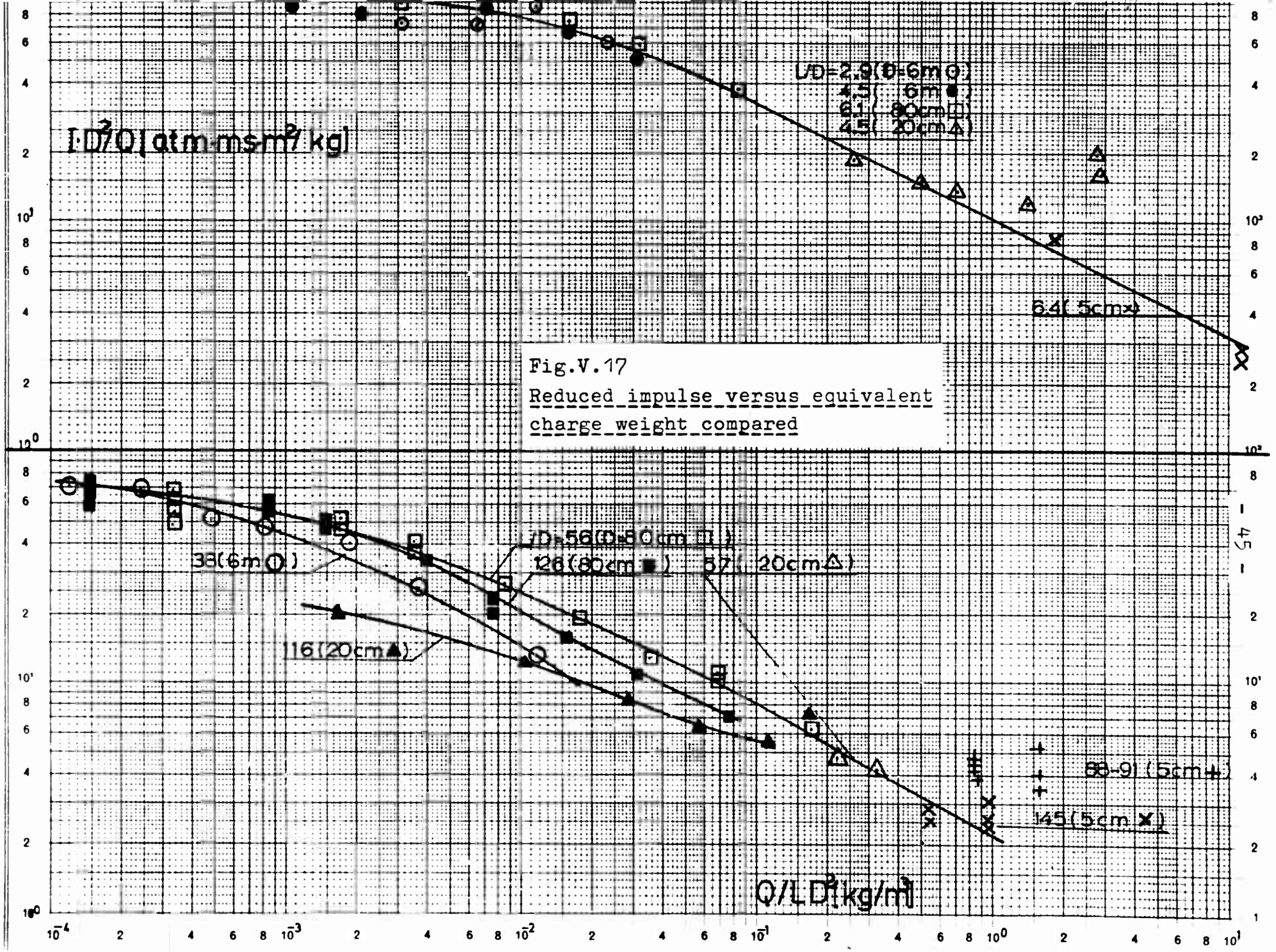

Fig.V.17
Reduced impulse versus equivalent charge weight compared

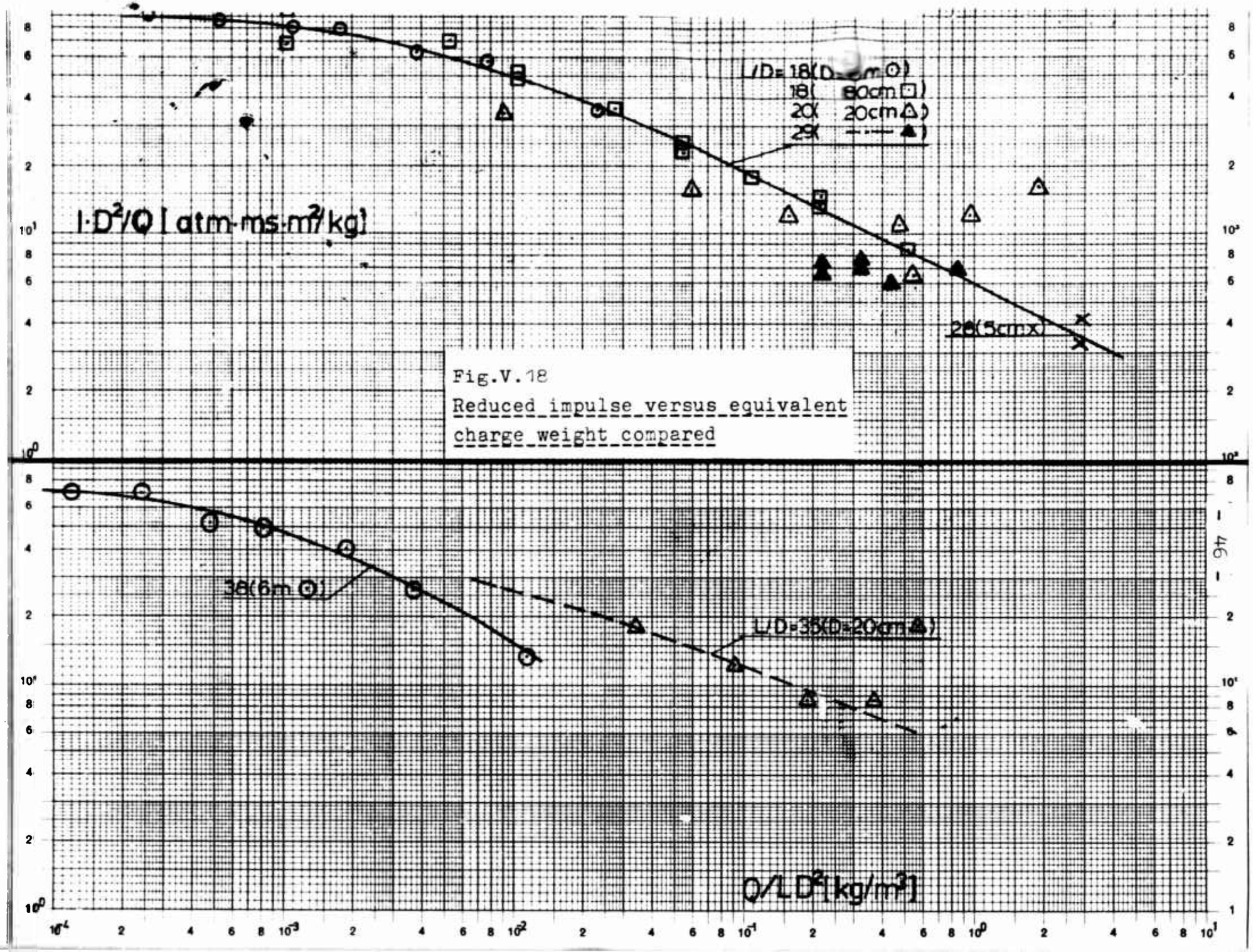

Fig.V.18
Reduced impulse versus equivalent charge weight compared

V.3 Positive duration

The scaling law proposed in chapter II.2 eq (II.11) for the positive duration t_+

$$(II.11)\quad \frac{t_+ \cdot D^2}{Q} = h\left(\frac{Q}{LD^2}\right) = h\,(Q_E)$$

is checked with experiments in fig V.19.

We are seeing the same tendency here as for the impulse - lowering of the reduced positive duration curves with increasing L/D values. The wall roughness seems not to have a simple scaled influence.

For $L/D \lesssim 7$ the positive duration seems to scale roughly for all tubes and tunnel.

We may propose here too that loading analysis be made utilizing the $L/D \lesssim 7$ data only to have a safety factor.

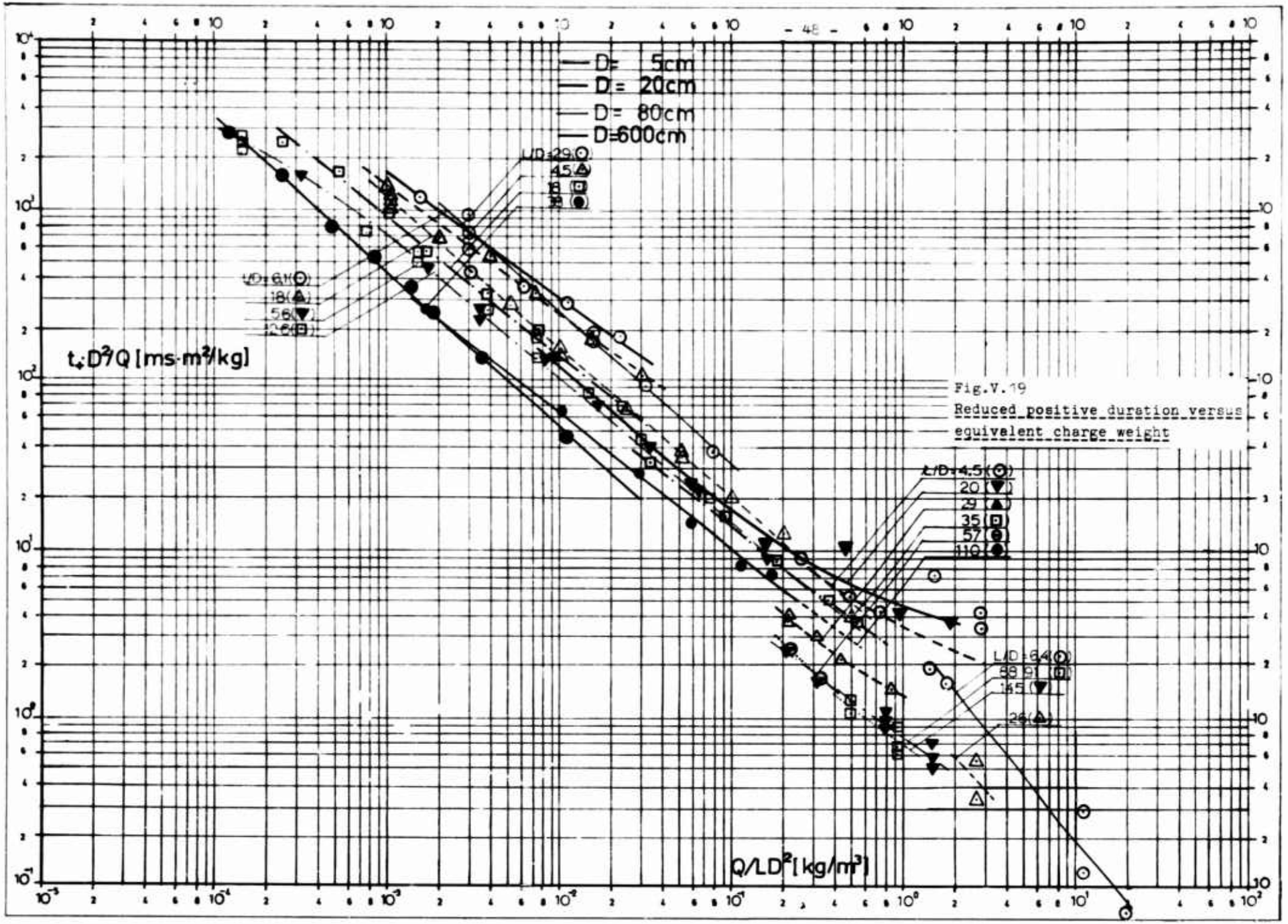

Fig.V.19
Reduced positive duration versus equivalent charge weight

V.4 Time of arrival

Time from detonation to blast wave reaches distance L, was found to scale as

$$(II.12)\quad \frac{t_a \cdot D^2}{Q} = i\ (\frac{Q}{LD^2}) = i\ (Q_E)$$

which is checked with the experiments in fig V.20 for all tubes and tunnel in rock. We have no significant deviation in this case from one smooth curve with increased L/D values within the experimental uncertainty

$$\text{For}\quad 10^{-5} \lesssim \frac{t_a D^2}{Q} \lesssim 10^{-2} \left[\frac{ms \cdot m^2}{kg}\right]$$

$$\text{and}\quad 10^{-5} \lesssim \frac{Q}{LD^2} \lesssim 10^{-2} \left[\frac{kg}{m^3}\right]$$

the scaled curve may roughly be described by the straight line in the log-log plot as:

$$(V.8)\quad \frac{t_a \cdot D^2}{Q} \simeq 2{,}05\ (\frac{Q}{LD^2})^{-1{,}05}$$

or

$$(V.9)\quad t_i(ms) \simeq 2{,}05\ \frac{D^{0{,}1} \cdot L^{1{,}05}}{Q^{0{,}05}}$$

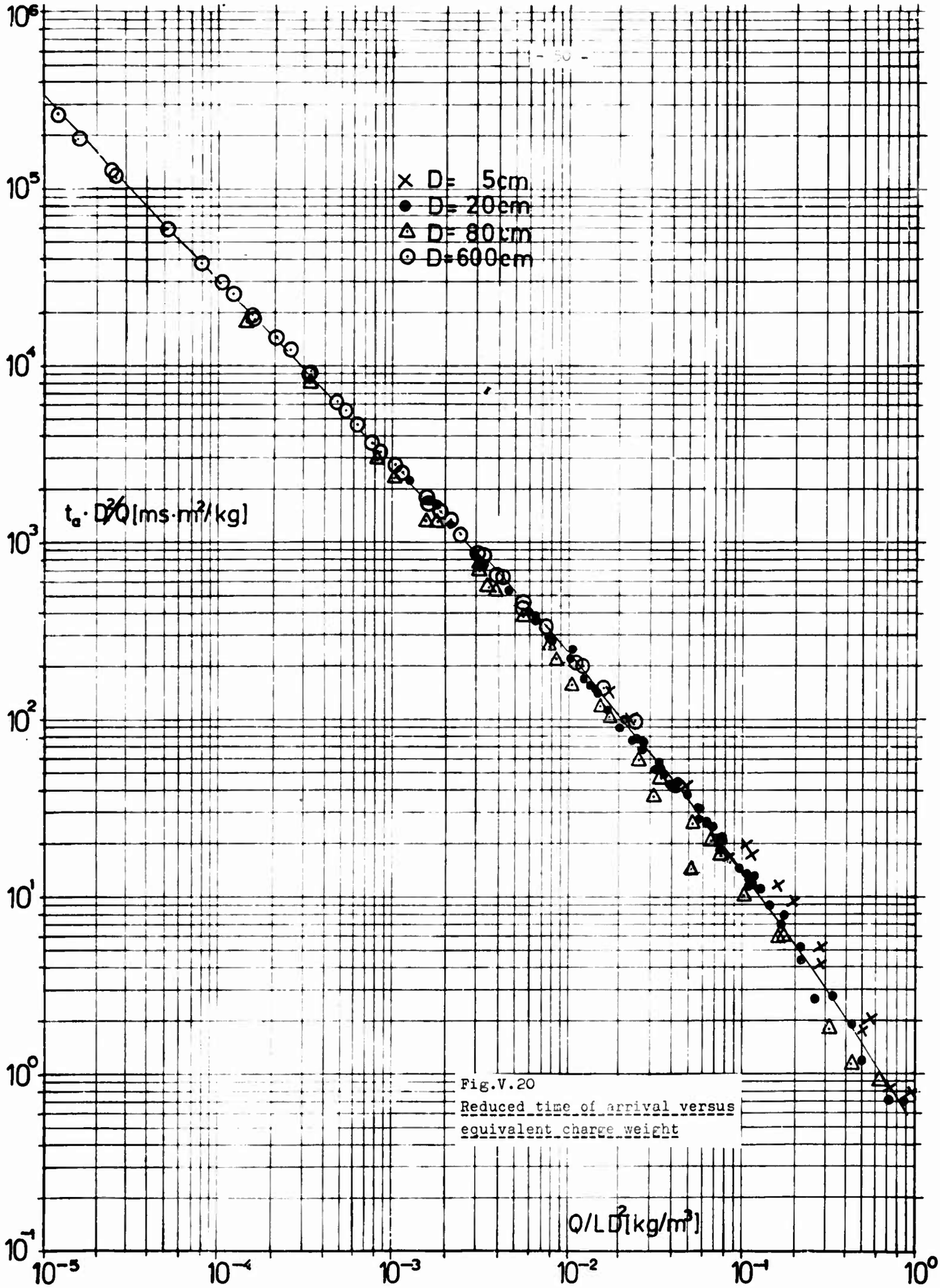

Fig.V.20
Reduced time of arrival versus equivalent charge weight

VI SUMMARY

Frontpressure of an one-dimensional blast wave generated by a charge detonating in a tunnel scales as

(VI.1) $$p = f\left(\frac{Q}{LD^2}\right)$$

with an attenuation dependent on wall roughness and L/D parameter. The average L/D influence on the "attenuation" from an "unattenuated" scaled pressure curve, $P_{so}(Q_E)$ $(L/D \rightarrow 0)$, is evaluated to be

(V.2) $$P = P_{so}\exp\left[-k(L/D)\right]$$

Estimates of k is given in fig V.13 for different tubes and tunnel in rock.

Typical for $p_{so} \simeq$ 1 atm, 5, 20 and 80 cm tubes with wall roughness 0,03 - 0,5% have

$k \simeq (4 \pm 2) \cdot 10^{-3}$.

For the 6 m diameter tunnel in rock, roughness $\gtrsim 8\%$, $k \simeq (3 \pm 1) \cdot 10^{-2}$.

The reduced impulse scales as

(VI.3) $$\frac{I \cdot D^2}{Q} = g\left(\frac{Q}{LD^2}\right)$$

with an L/D influence dependent on roughness similar to frontpressure.

The reduced positive duration scales as

(VI.4) $$\frac{t_+ \cdot D^2}{Q} = h\left(\frac{Q}{LD^2}\right)$$

with similar effects as described above.

The reduced time of arrival scales as

$$(VI.5) \quad \frac{t_a \cdot D^2}{Q} = i\left(\frac{Q}{LD^2}\right)$$

which does not seem to have a significant L/D dependence

For $10^{-5} \lesssim \frac{Q}{LD^2} \lesssim 10^{-2}$

$$t_a(ms) \simeq 2{,}05 \frac{D^{0,1} \cdot L^{1,05}}{Q^{0,05}}$$

with D(m)
L(m)
Q(kg TNT)

It is recommended that loading analysis to be made utilizing the "smooth tube" or lim $L/D \rightarrow 0$ data only. It is felt that, although roughness does not seem to scale, any roughness in a tunnel would tend to be a safety factor if doors, equipment etc are designed to withstand "smooth wall" loads.

The "smooth wall" reduced parameters for the blast wave are presented in fig VI.1 with rough estimates of the uncertainty.

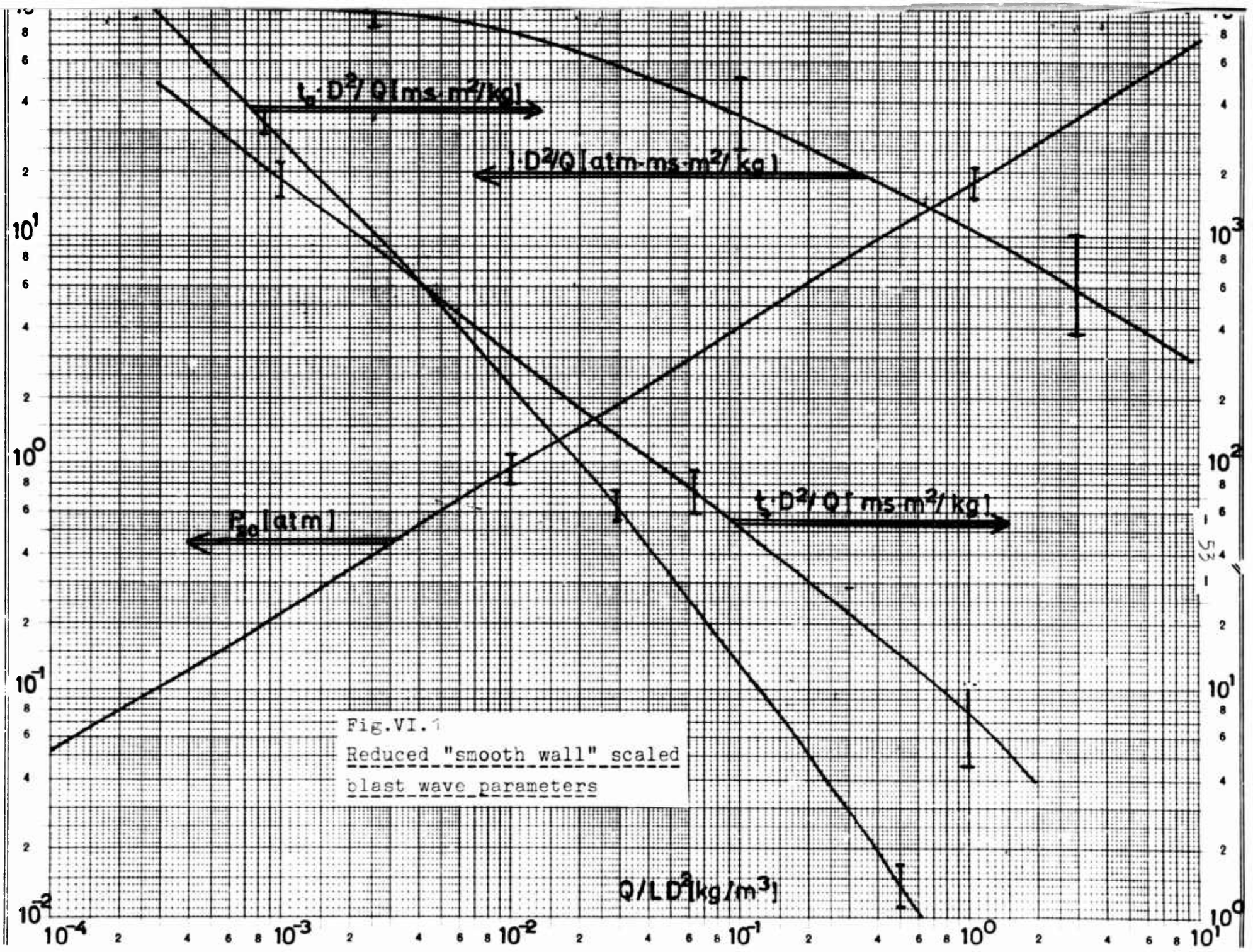

Fig.VI.1
Reduced "smooth wall" scaled blast wave parameters

REFERENCES

/1/ Langhaar, H.L.

"Dimensional Analysis and Theory of Models".
John Wiley & Sons, Inc (1951)

/2/ Cole, R.H.

"Underwater explosions"
Dover Publications, Inc.

/3/ Eriksson, S.

"Fronttryck ock impuls hos endimensionell stötvåg vid detonation i tunnel."

(Front pressure and impuls of an one-dimensional shock wave generated by a charge detonation in a tunnel).

Report no 103.35 Royal Swedish Administration of Fortification. (1964).

/4/ Emerich, R.J. and Curtis, C.W.

"Attenuation in shock tube".
Journal of Applied Physics 24, 360 (1953).

/5/ Curran, D.R.

"Underground storage of ammunition.
Experiments concerning accidental detonation in an underground chamber."

Internal report no X-III.

Norwegian Defence Research Establishment (1966).

/6/ Jenssen, A. - Michalsen, H and Sølvberg, A.

"Sikkerhetsspørsmål ved ammunisjonslagre."
Fortifikatorisk notat nr 26/65.
Norwegian Defence Construction Service (1965).